

# A role for post-transcriptional control of endoplasmic reticulum dynamics and function in *C. elegans* germline stem cell maintenance

Richa Maheshwari<sup>1</sup>, Kumari Pushpa<sup>1</sup> and Kuppuswamy Subramaniam<sup>1,2,\*</sup>

## ABSTRACT

Membrane-bound receptors, which are crucial for mediating several key developmental signals, are synthesized on endoplasmic reticulum (ER). The functional integrity of ER must therefore be important for the regulation of at least some developmental programs. However, the developmental control of ER function is not well understood. Here, we identify the *C. elegans* protein FARL-11, an ortholog of the mammalian STRIPAK complex component STRIP1/2 (FAM40A/B), as an ER protein. In the *C. elegans* embryo, we find that FARL-11 is essential for the cell cycle-dependent morphological changes of ER and for embryonic viability. In the germline, FARL-11 is required for normal ER morphology and for membrane localization of the GLP-1/Notch receptor involved in germline stem cell (GSC) maintenance. Furthermore, we provide evidence that PUF-8, a key translational regulator in the germline, promotes the translation of *farl-11* mRNA. These findings reveal that ER form and function in the *C. elegans* germline are post-transcriptionally regulated and essential for the niche-GSC signaling mediated by GLP-1.

**KEY WORDS:** Self-renewal, Differentiation, STRIPAK, Far complex, Germ cells

## INTRODUCTION

Endoplasmic reticulum (ER) is the site of synthesis and folding of all secreted and transmembrane proteins, including the ligands and receptors of some key signaling pathways. Not surprisingly, ER malfunction is associated with many human diseases, including diabetes, Alzheimer's disease and cancer (Hoozemans et al., 2006; Jamora et al., 1996; Scheuner et al., 2005). The ER is an extended, membrane-bound organelle with a continuous lumen. Its local morphology has distinct features, such as tubules, flattened sheet-like cisternae and the nuclear envelope (NE). Each of these ER subdomains appears to be particularly suited to specific functions. For example, rough ER engaged in protein synthesis is mainly composed of sheets, whereas the smooth ER involved in lipid synthesis is primarily made of tubules. Perhaps as a consequence of this division of labor, ER adopts mostly a sheet-like structure in protein-secreting cells and a tubular form in steroid-exporting cells (Shibata et al., 2006). Thus, proper ER morphology is crucial for the functional specialization of the various cell types.


The ER constantly remodels itself, with the tubules and sheets continuously forming and collapsing. Since the NE disassembles and reassembles during cell division, the morphological changes of ER are particularly dramatic in dividing cells (Du et al., 2004; Puhka et al., 2007; Wang et al., 2013). Predictably, several proteins involved in the maintenance of ER morphology have essential roles during cell division, which suggests that the ability of ER to change its morphology might be crucial for proper cell division (Audhya et al., 2007; Bonner et al., 2013; Schlaitz et al., 2013). Therefore, at least some of the signals that control cell proliferation most likely influence ER dynamics. Consistent with this notion, the Target of rapamycin complex 1 (TORC1) signaling pathway has recently been shown to be essential for normal ER morphology and homeostasis in *Drosophila* cells (Sanchez-Alvarez et al., 2014). However, the developmental control of ER dynamics is still largely unexplored.

RNA-binding proteins of the PUF family function as key translational regulators in a number of developmental processes (Forbes and Lehmann, 1998; Lehmann and Nusslein-Volhard, 1987; Souza et al., 1999; Walser et al., 2006; Zhang et al., 1997). Although some of their functions are species specific, the role of PUF proteins in the control of germline stem cell (GSC) proliferation is conserved across species (Crittenden et al., 2002; Forbes and Lehmann, 1998; Xu et al., 2007). *C. elegans* PUF-8 regulates several aspects of germ cell development, including GSC proliferation, mitotic-to-meiotic transition, spermatogenesis-to-oogenesis switch in hermaphrodites and the meiotic progression of spermatocytes (Ariz et al., 2009; Bachorik and Kimble, 2005; Priti and Subramaniam, 2015; Racher and Hansen, 2012; Subramaniam and Seydoux, 2003; Vaid et al., 2013).

A genetic screen had previously isolated several mutant alleles as enhancers of the *puf-8* phenotype (M. Ariz, PhD thesis, Indian Institute of Technology Kanpur, 2010; Vaid et al., 2013). We have now mapped one of them to *farl-11*, which encodes the *C. elegans* ortholog of yeast FAR11 and the mammalian striatin-interacting protein isoforms 1 and 2 (STRIP1/2). FAR11 and STRIP1/2 are components of a phosphatase-kinase complex known as the FAR complex in yeast and the STRIPAK complex in mammals (Hwang and Pallas, 2014). Our results reveal that PUF-8 promotes the germline expression of FARL-11, and that FARL-11 contributes to GSC proliferation by promoting GLP-1/Notch signaling. Further, we find that the *C. elegans* FARL-11, like its yeast counterpart FAR11, is localized on ER (Pracheil and Liu, 2013). Additionally, removal of FARL-11 alters ER morphology and considerably reduces the membrane localization of GLP-1, suggesting that FARL-11 is essential for ER form and function. These results show that the ER localization of FARL-11 has been conserved in evolution and provide evidence that the modulation of ER dynamics

<sup>1</sup>Department of Biological Sciences and Bioengineering, Indian Institute of Technology, Kanpur 208016, India. <sup>2</sup>Department of Biotechnology, Indian Institute of Technology – Madras, Chennai 600036, India.

\*Author for correspondence (subbu@iitm.ac.in)

 K.S., 0000-0002-1691-489X

is one of the mechanisms by which factors such as the PUF proteins regulate development.

## RESULTS

### Maternal FARL-11 is essential for embryonic and larval development

Although *puf-8* participates in several events during germ cell development, worms homozygous for the null alleles of *puf-8*, such as *puf-8(zh17)*, are fertile at 20°C and sterile only at 25°C. Taking advantage of this feature, a genetic screen was previously carried out for enhancer mutations, which isolated a number of mutant alleles that are sterile at 20°C only in combination with *puf-8(zh17)* (M. Ariz, PhD thesis, Indian Institute of Technology Kanpur, 2010; Vaid et al., 2013). We have now mapped one such allele, *kp35*, to the *farl-11* locus using standard three-factor mapping, sequence comparison, RNAi and transgene rescue (see the supplementary Materials and Methods for details). The protein encoded by *farl-11* (factor arrest-like-11) shares a high degree of sequence similarity with yeast FAR11 and the human STRIP1 and STRIP2 (also known as FAM40A and FAM40B) proteins (Fig. S2) (Kemp and Sprague, 2003).

The FAR/STRIPAK complex is involved in various cellular processes, including vesicular trafficking/dynamics, cell migration, cell cycle control and signaling (Hwang and Pallas, 2014; Lant et al., 2015). Nevertheless, the characterization of a loss-of-function phenotype using a genetic mutant allele has not yet been reported for a metazoan ortholog of *farl-11*. Therefore, we first focused on the *farl-11(kp35)* single-mutant phenotype. Embryos homozygous for the *kp35* allele from *farl-11(kp35/+)* heterozygous hermaphrodites were viable; they hatched and developed normally into fertile adults. However, the *farl-11(kp35/kp35)* homozygous adults produced fewer embryos than the wild type, and ~40% of these embryos did not hatch; the remainder failed to progress through the larval stages (Fig. S3D,F). These results show that maternally provided FARL-11 is essential for embryogenesis and larval development and suggest that FARL-11 activity might be crucial for both cell proliferation and differentiation.

### GSCs are lost in the *farl-11 puf-8* double mutant

The reduced brood size of *farl-11(kp35)* worms prompted us to examine their germlines. The adult *C. elegans* germline is polarized on a distal-proximal axis, with GSCs at the distal end. Germ cells

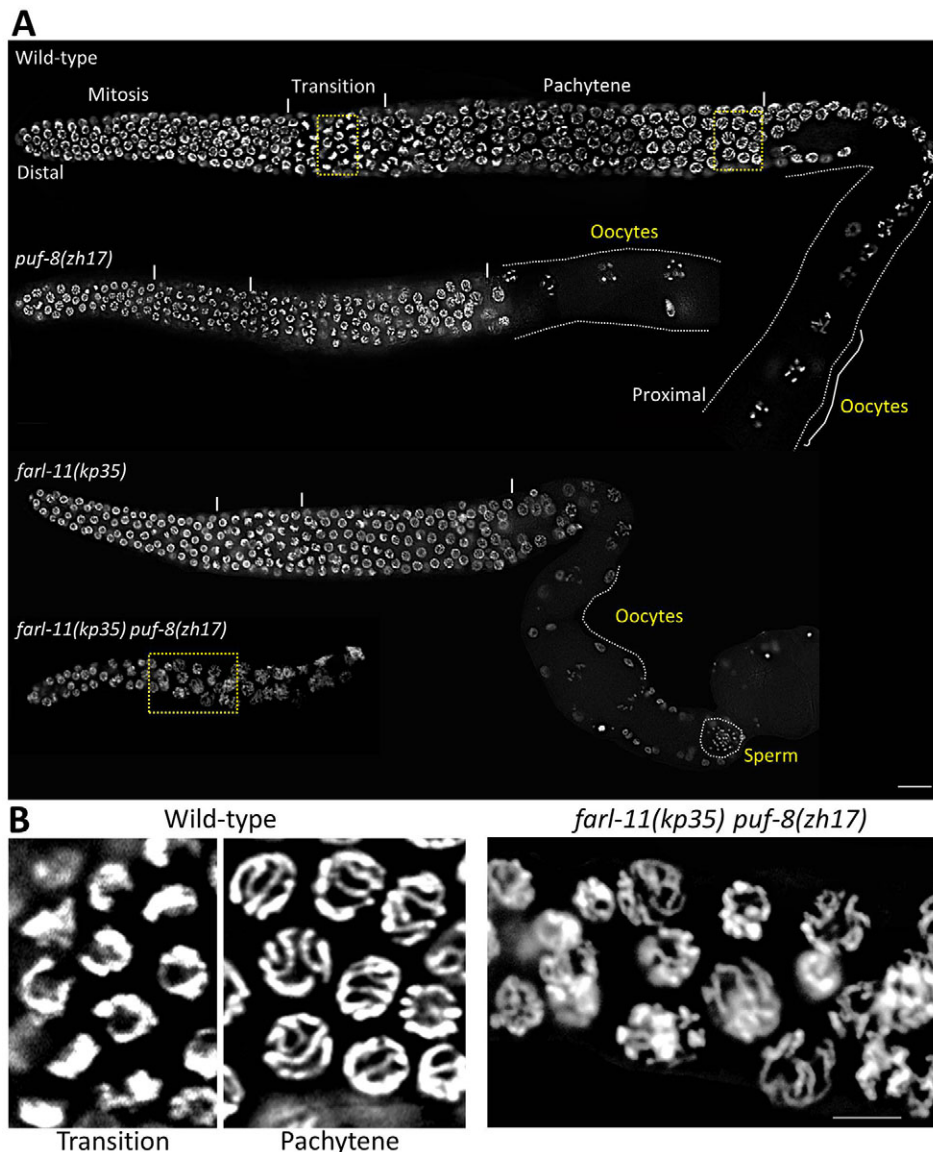


**Fig. 1. *farl-11 puf-8* double-mutant worms do not produce gametes.** (A) Gonads dissected from adult hermaphrodites and stained with DAPI are shown at the same magnification. In this and subsequent figures, the distal mitotic region is to the left and the proximal region containing gametes is to the right. Regions of the germline with germ cells at different stages of development are marked with solid white lines and are labeled in the image of wild type. In wild type and *puf-8(zh17)* (strain IT60), the proximalmost part of the gonad containing sperm is not visible in these images. Neither type of gametes is present in the *farl-11 puf-8* (strains IT73 and IT175) double-mutant germline. (B) Higher magnification of boxed regions in A showing germline chromatin morphology. Note that the *farl-11 puf-8* double-mutant chromatin lacks the morphology characteristic of normal meiotic stages. Scale bars: 20  $\mu$ m in A; 5  $\mu$ m in B.

enter and progress through meiosis as they move proximally. As a consequence of this arrangement, the mature gametes are found in the proximal part (Fig. 1A). The *farl-11(kp35)* germlines, when compared with the wild type, were smaller and contained fewer germ cells in the mitotic and pachytene zones (Fig. 1A and see Fig. 8A). However, the *farl-11(kp35)* germlines did produce both types of gametes (Fig. 1A). By contrast, the overall size of *farl-11(kp35) puf-8(zh17)* germlines was severely reduced, and these germlines produced neither sperm nor oocytes (Fig. 1A). In the wild-type germline, chromatin assumes a distinct morphology at each stage of meiosis that is characteristic of that particular stage. The *farl-11 puf-8* double-mutant chromatin did not possess any of these characteristic morphologies; instead, it appeared as loosely folded thin fibers in the proximal germline (Fig. 1B).

In the wild type, actively dividing germ cells, as judged by immunostaining for the metaphase marker phospho-histone H3 (PH3), are found in the distal part of the germline. Cells in this region do not express the meiotic marker HIM-3 (Zetka et al., 1999). In the *farl-11(kp35)* germlines, although there was a significant reduction in the number of actively dividing cells, no HIM-3-positive cells were present in the distal germline (Fig. 2). By contrast, in the *farl-11 puf-8* double-mutant germlines, HIM-3 was present on chromatin even in the distalmost germ nuclei in adults, although it was excluded from the mitotic chromatin in larvae (Fig. 2A). Consistently, the number of PH3-positive cells was drastically reduced in the *farl-11 puf-8* double-mutant germlines at both L4 and adult stages (Fig. 2B,C; Fig. S4). Together, these results point to two distinct germ cell defects in the double mutant: (1) the germ cells that enter meiosis during the larval stage fail to progress through meiotic development; and (2) GSCs fail to self-renew and are lost due to premature meiotic entry.

### *kp35* is a hypomorphic allele of *farl-11*

*kp35* is a missense mutation that replaces serine 169 with a leucine (Fig. S1). Serine at position 169 is only partially conserved, and the N-terminal region that contains serine 169 is less conserved than the highly conserved C-terminal region (Fig. S2). These observations prompted us to test whether *kp35* is a hypomorphic allele by complementation with a null allele; however, the only other available allele, *tm6233*, also appears to be hypomorphic (Fig. S3). As an alternative strategy, we depleted FARL-11 by RNAi in *farl-11(kp35/kp35)* worms. Whereas the *farl-11(kp35/kp35)* homozygous progeny of *farl-11(kp35/+)* heterozygous worms were all fertile at 25°C, *farl-11(kp35/kp35)* worms depleted of FARL-11 by RNAi were all sterile at this temperature, suggesting that *kp35* is a hypomorphic allele (Fig. S3E). Since *farl-11* does not share significant similarity with any other *C. elegans* gene, it is unlikely that the sterile phenotype resulted from an off-target effect of RNAi.

### MEX-3 and PUF-8 function redundantly to promote *farl-11* 3' UTR-mediated expression in mitotic germ cells

Since PUF-8 is a translational regulator, it is possible that it promotes FARL-11 expression and that the *farl-11 puf-8* double-mutant phenotype actually results from the reduced expression of a functionally weaker FARL-11. PUF-8 mediates its translational control activity via the 3' UTR sequences of its targets (Mainpal et al., 2011; Vaid et al., 2013). As a first step to test our hypothesis, we examined whether PUF-8 could promote *farl-11* 3' UTR-mediated expression of a GFP::H2B reporter in the germline using a previously described 3' UTR reporter assay (D'Agostino et al., 2006). In the wild-type genetic background, GFP::H2B was

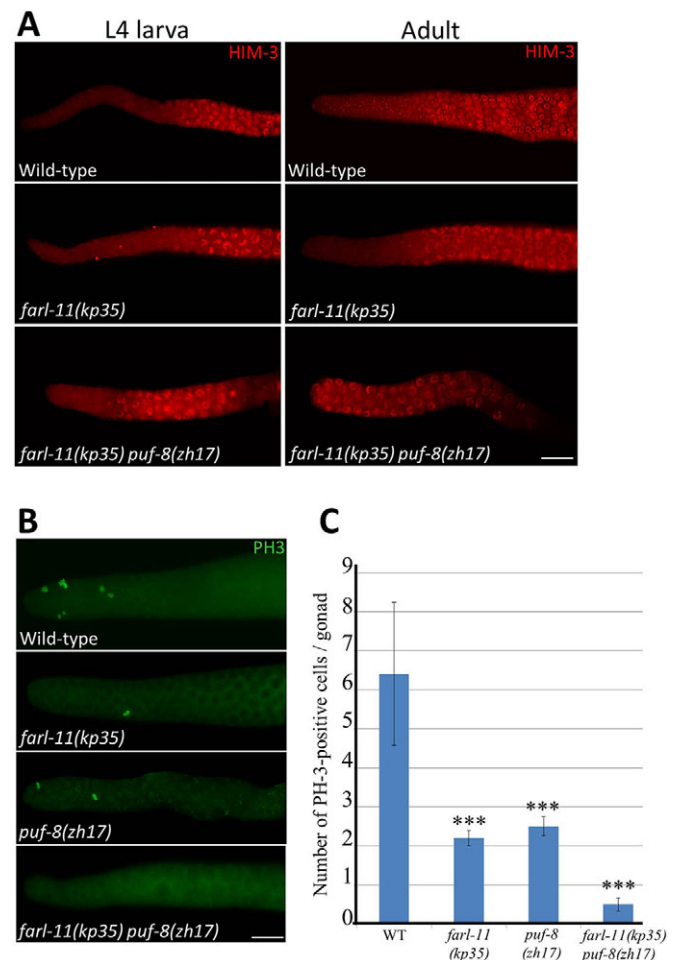


**Fig. 2. Germline stem cells are absent in *farl-11 puf-8* double-mutant adult germlines.** (A) Gonads were dissected at the stages indicated from hermaphrodites of the indicated genotypes and immunostained for the meiotic marker HIM-3. Note the presence of HIM-3 on chromatin in the distal region of the *farl-11 puf-8* (strains IT73 and IT175) double-mutant germline; this region normally contains mitotically cycling germ cells, which lack HIM-3 on the chromatin. A few bright dots of fluorescence seen in *farl-11* L4 (strain IT719) and wild-type adult germlines are technical artefacts. (B) Adult germlines immunostained for the mitotic marker phospho-histone H3 (PH3). (C) Quantitation of immunostaining with anti-PH3 antibody. Error bars indicate s.d. \*\*\* $P < 0.0001$  (Student's *t*-test) for wild type (WT) versus each mutant. Scale bars: 20  $\mu$ m.

strongly expressed in the distal germline. It decreased gradually in more proximal regions, reaching the lowest levels around the mid-pachytene region. GFP::H2B levels began to rise again in the region where cells exit pachytene and reached the highest levels in oocytes (Fig. 3A). By contrast, GFP::H2B expression in the distal region was significantly reduced in worms lacking PUF-8 (Fig. 3B), indicating that PUF-8 is required for robust expression of the *farl-11* 3' UTR reporter in mitotic germ cells. Comparison of *farl-11* mRNA levels between *puf-8(+/-)* and *puf-8(-/-)* animals did not reveal any significant difference, which is consistent with a post-transcriptional role for PUF-8 in *farl-11* expression (Fig. 3C).

Like PUF-8, the KH-domain RNA-binding protein MEX-3 is also highly expressed in the distal germline, and MEX-3 and PUF-8 function redundantly to promote the mitotic proliferation of germ cells (Ariz et al., 2009; Ciosk et al., 2004). We tested whether *farl-11* 3' UTR reporter expression in the distal germline was also



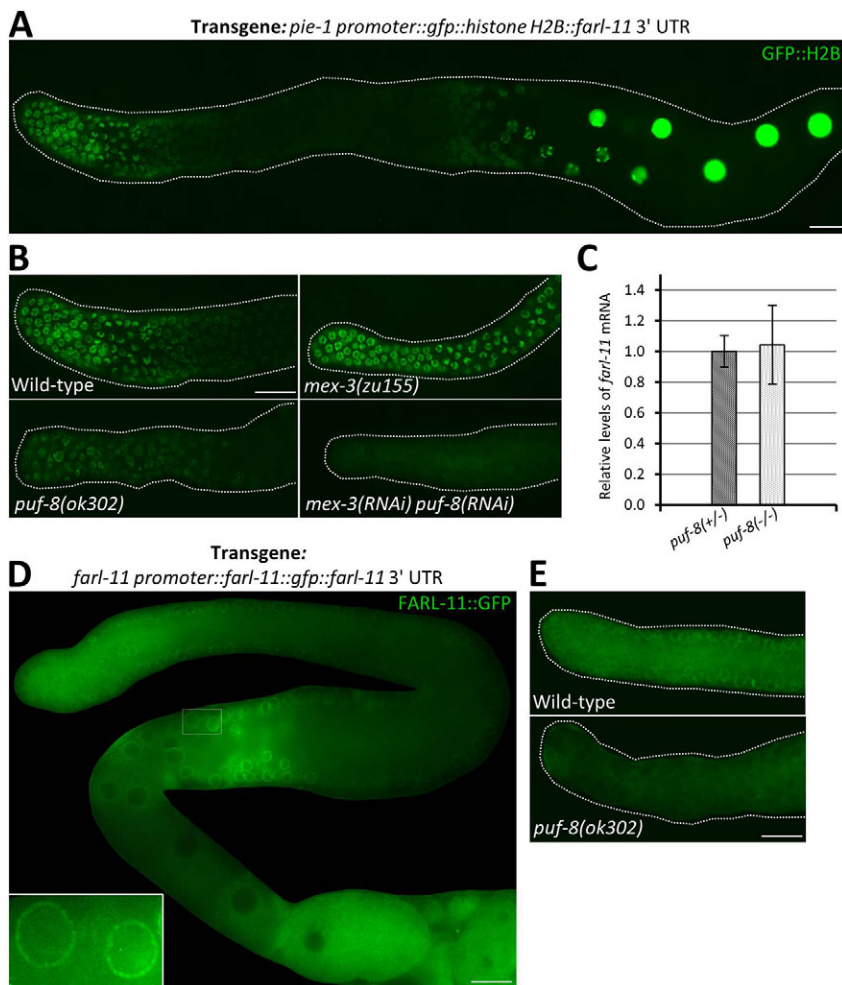


**Fig. 3. PUF-8 promotes FARL-11 expression in mitotic germ cells.** (A) Expression pattern of GFP::H2B in a transgenic hermaphrodite carrying the indicated transgene (strain IT729). (B) Expression pattern of the same transgene as in A in the distal germline of worms of the indicated genotypes or following RNAi treatment (strains IT729, IT735 and IT767). (C) Comparison of *farl-11* mRNAs between *puf-8(+/-)* and *puf-8(-/-)* worms quantitated by real-time RT-PCR. Four biological replicates and eight technical replicates were used for the quantitation.  $P=0.6718$  [Student's *t*-test for *puf-8(+/-)* versus *puf-8(-/-)*]. (D) Expression pattern of the FARL-11::GFP fusion protein in a transgenic worm carrying the indicated transgene (strain IT807). Inset reveals the localization of FARL-11::GFP on the nuclear envelope (NE). (E) Comparison of expression of the same transgene as in D between wild-type (strain IT807) and *puf-8(-)* (strain IT853) genetic backgrounds in the distal germline. Note that the perinuclear localization of FARL-11::GFP observed in the wild type is drastically reduced in the *puf-8(-)* germline. Scale bars: 20  $\mu$ m.

dependent on MEX-3. Surprisingly, we did not observe any difference in GFP::H2B levels between the *mex-3* mutant and control worms. However, this might not rule out a role for MEX-3 in the translational regulation of *farl-11*, as the presence of PUF-8 alone could be sufficient for normal levels of *farl-11* 3' UTR reporter expression. We therefore tested whether the removal of both MEX-3 and PUF-8 has a greater effect on reporter expression than removal of PUF-8 alone. Worms homozygous for null alleles of *mex-3* and *puf-8* [*mex-3(zu155); puf-8(zh17)*] have severely underproliferated germlines, which made observation of GFP expression in these worms difficult. Therefore, we partially depleted both MEX-3 and PUF-8 by RNAi, which has been shown to masculinize the hermaphrodite germline but not affect germ cell proliferation (Ariz et al., 2009). As shown in Fig. 3B, RNAi-mediated depletion of MEX-3 and PUF-8 completely abolished *farl-11* 3' UTR reporter expression. This is unlikely to be due to a global failure of translation in the *mex-3(RNAi); puf-8(RNAi)* worms because the expression of other 3' UTR reporters was unaffected in these worms (Fig. S5). These results indicate that MEX-3 and PUF-8 may function redundantly to promote the translation of *farl-11* mRNA in the distal germline.

Next, we examined whether the expression of endogenous FARL-11 is also dependent on PUF-8 and/or MEX-3. Since no FARL-11-specific antibodies were available, we generated transgenic lines that express FARL-11 as a GFP fusion (FARL-11::GFP) under the control of the *farl-11* promoter and 3' UTR sequences. Similar to the *farl-11* 3' UTR reporter, FARL-11::GFP

was more strongly expressed in the distal mitotic zone than in the pachytene zone (Fig. 3D). Expression of FARL-11::GFP was unaffected by the removal of MEX-3 (data not shown), whereas depletion of PUF-8 nearly abolished FARL-11::GFP expression in the distal germline (Fig. 3E). These results support the contention that PUF-8 promotes FARL-11 expression in the distal germline.

#### PUF-8 interacts with *farl-11* mRNA in vivo and the *farl-11* 3' UTR in vitro

PUF-8 has been shown to control translation by direct 3' UTR binding (Mainpal et al., 2011; Vaid et al., 2013). Previously, a fusion protein containing PUF-8, nine repeats of the HA epitope and GFP (PUF-8::9xHA::GFP) had been shown to co-immunoprecipitate with *let-60* mRNA from transgenic worm lysates (Vaid et al., 2013). Following the same strategy, we immunoprecipitated (IP) the PUF-8::9xHA::GFP fusion protein using anti-HA antibodies from whole worm lysates and examined the IP pellet for the presence of *farl-11* mRNA by RT-PCR. Amplification with *farl-11*-specific PCR primers yielded products of the expected size from RNA extracted from the lysate as well as from the IP pellet. By contrast, primers specific for *pie-1*, which was used as a negative control, failed to amplify any specific PCR product from the IP pellet (Fig. 4A). These results indicate that PUF-8 either directly interacts with, or is present in a complex containing, the *farl-11* mRNA.

We performed electrophoretic mobility shift assays (EMSAs) to distinguish between the above two possibilities. A bacterially

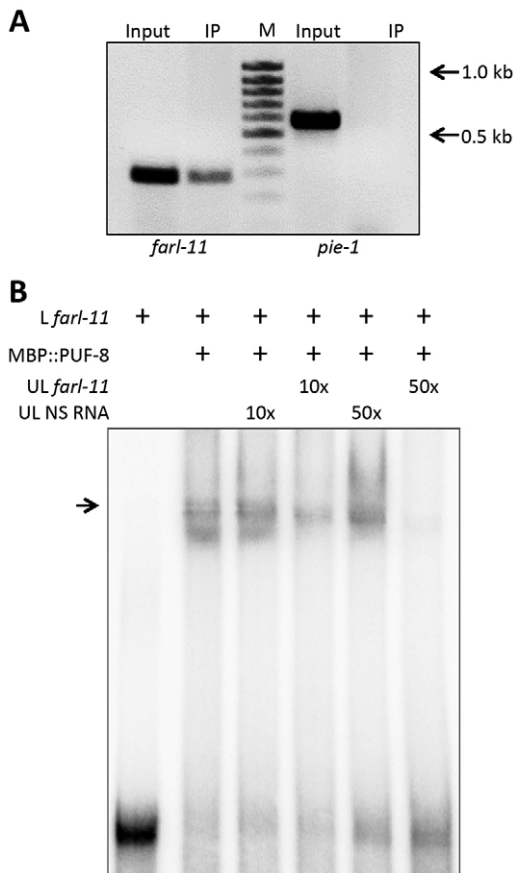


**Fig. 4. PUF-8 interacts with the *farl-11* 3' UTR.** (A) Co-immunoprecipitation assay. PUF-8::9xHA::GFP fusion protein from the lysate of transgenic worms (strain IT722) was immunoprecipitated with anti-HA antibodies. Co-immunoprecipitation of the indicated RNAs was detected by RT-PCR. *pie-1* mRNA was used as a negative control. Input, RT-PCR product amplified from RNA extracted from the same volume of lysate as used for IP; IP, RT-PCR product amplified from the immunoprecipitate pellet; M, molecular weight markers. (B) EMSA patterns of radiolabeled *farl-11* 3' UTR RNA (L *farl-11*) in the presence of the indicated components. MBP::PUF-8 is a bacterially expressed fusion protein containing maltose-binding protein and the PUF domain (amino acids 175–535) of PUF-8. UL, non-radiolabeled; NS, a non-specific control RNA of ~200 nucleotides; 10× and 50× indicate 10-fold and 50-fold molar excess compared with the radiolabeled RNA. Arrow indicates the mobility shifted band.

expressed fusion protein containing maltose-binding protein and the PUF domain (amino acids 175–535) of PUF-8 (MBP::PUF-8) has been shown to specifically interact with *pal-1* and *let-60* 3' UTRs in EMSAs (Mainpal et al., 2011; Vaid et al., 2013). We performed similar assays and found that the MBP::PUF-8 fusion protein retarded the mobility of radiolabeled *farl-11* 3' UTR RNA. Even the presence of a 50-fold molar excess of an unlabeled RNA, unrelated in sequence to that of the *farl-11* 3' UTR, did not affect the mobility shift. By contrast, the addition of a 10-fold molar excess of unlabeled *farl-11* 3' UTR RNA considerably weakened, and a 50-fold molar excess completely abolished, the mobility shift of the radiolabeled version (Fig. 4B; Fig. S6). These results show that PUF-8 is capable of directly binding to the *farl-11* 3' UTR in a sequence-specific manner.

Together, the results of the 3' UTR reporter expression, co-IP and EMSAs strongly suggest that PUF-8 promotes the translation of *farl-11* mRNA in the distal germline by directly interacting with the *farl-11* 3' UTR.

### FARL-11 is an ER protein

In the transgenic lines described above, FARL-11::GFP appeared to be localized on the NE of germ cells (Fig. 3D). We generated a double-transgenic line expressing FARL-11::GFP and the NE marker mCherry::EMR-1, and found that FARL-11::GFP was indeed localized on the NE (see Fig. 6A). FARL-11::GFP expression was also observed in embryos, where its distribution underwent dramatic changes during the cell division cycle (Fig. 5). During the meiotic metaphase, FARL-11::GFP was localized on centrosomes and in certain clusters in the cortex. Similar association with centrosomes was also observed during the mitotic metaphase. During mitotic telophase, in addition to being on centrosomes, FARL-11::GFP was present in the space between the two nascent daughter nuclei. Occasionally, FARL-11::GFP was found in small clusters in the cytoplasm at this stage. It began to accumulate prominently on the centrosomes again during anaphase, and formed a mesh-like arrangement around the interphase nucleus. This dynamic distribution pattern is reminiscent of the dynamic changes in ER during the cell cycle (Poteryaev et al., 2005), which prompted us to check whether FARL-11::GFP is localized on ER. Although the NE is contiguous with the rough ER, not all NE proteins are present on the cytoplasmic ER network. Therefore, we generated double-transgenic lines expressing FARL-11::GFP and mCherry::SP12, which is a marker for ER (Joseph-Strauss et al., 2012), and examined the distribution patterns of both proteins in germlines and embryos. As shown in Fig. 6, FARL-11::GFP showed strong colocalization with mCherry::SP12 in the germline as well as in the embryo at different stages of the cell cycle, indicating that FARL-11 might indeed be localized on ER, like the yeast FAR complex (Pracheil and Liu, 2013).

### *farl-11* is required for ER integrity

To determine whether FARL-11 plays any role in ER morphology and/or function, we observed ER morphology in live worms using the GFP::SP12 reporter (Poteryaev et al., 2005). Whereas the distribution pattern of GFP::SP12 in the wild type was similar to that described above for mCherry::SP12, it was significantly altered in *farl-11* (*kp35*) germlines and embryos. In contrast to the uniform reticular arrangement of ER observed in the lumen of wild-type germlines, GFP::SP12 formed distinct, large patches in the lumen of *farl-11* mutant germlines. Similar large patches were observed in 66% of *farl-11* mutant embryos ( $n=80$ ) during both meiotic and mitotic metaphase stages (Fig. 7A), although these patches largely disappeared following the completion of cell division, at least in the one-cell embryo (Movies 1 and 2). We did not observe such large cytoplasmic ER patches in wild-type embryos (0/186). Further, we observed similar large cytoplasmic patches in *farl-11* (*kp35*) embryos using the NE marker mCherry::EMR-1 (Fig. 7B). These observations clearly show that FARL-11 is essential for normal ER morphology in both germline and embryo. In addition, we found that RNAi-mediated depletion of CASH-1, which is the *C. elegans* ortholog of yeast Far8 and the human striatins STRN, STRN3 and STRN4, caused similar ER defects to the *farl-11* mutation (Fig. S7). These results indicate that normal ER dynamics requires an intact FAR complex, and not just FARL-11 alone.

Since PUF-8 promotes FARL-11 expression (see above), we checked whether *puf-8* mutant animals also display ER defects. For this, we introduced the GFP::SP12 transgene into *puf-8* (*zh17*) worms and observed the dynamics of GFP::SP12 distribution during embryonic cell divisions as well as in the germline. In contrast to *farl-11* (*kp35*) germlines, GFP::SP12 did not show any significant aggregations in *puf-8* (*zh17*) germlines. However, in 45%



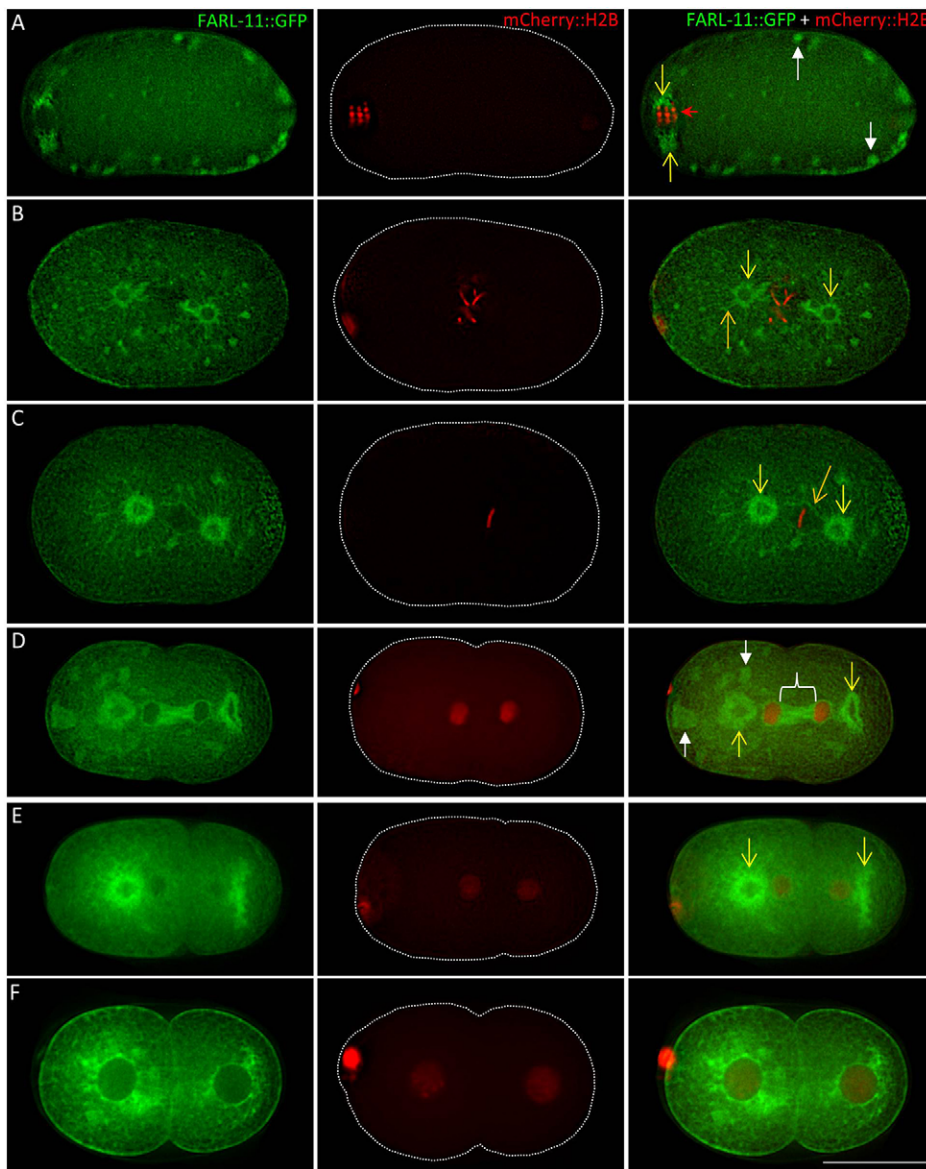


**Fig. 5. Dynamic localization pattern of FARL-11::GFP during the embryonic cell division cycle.** Changes in FARL-11 distribution were tracked during first cleavage using the FARL-11::GFP and mCherry::H2B reporter fusions (strain IT940). (A) Oocyte pronucleus in meiotic metaphase I (red arrow). (B–F) Different stages of the first mitotic division of the embryo. FARL-11::GFP localizes around centrosomes throughout the division cycle (yellow arrows); in addition, it appears as small cytoplasmic patches at the cortex during oocyte meiotic metaphase (white arrows) and seems to localize on astral and spindle microtubules during mitotic metaphase (orange arrows) (B,C). At anaphase, FARL-11::GFP forms a bridge-like band between the two daughter nuclei (bracket) (D). At metaphase and anaphase, FARL-11::GFP is distributed in patches in the cytoplasm (white arrows) as well in a few embryos (20%,  $n=50$ ). (E) At telophase, the cytoplasmic patches and the bridge-like band disappear; FARL-11::GFP emanates as thin tubes from around centrosomes, where its localization is more prominent. (F) At interphase, FARL-11::GFP forms a halo around the nucleus and is distributed as thin fibers throughout the cytoplasm. Scale bar: 20  $\mu\text{m}$ .

of *puf-8(zh17)* embryos ( $n=164$ ), large cytoplasmic patches of GFP::SP12 were observed during the meiotic and mitotic metaphase stages (Fig. 7; Movie 3), indicating that PUF-8 is required for normal ER dynamics in the embryo. Since the expression of FARL-11::GFP was reduced in the *puf-8* mutant germlines (Fig. 3E), the oocytes in these germlines probably accumulate insufficient FARL-11 to achieve normal ER dynamics in the embryo. However, these results do not rule out the possibility that *puf-8* contributes to ER dynamics in the embryo through an unknown mechanism that is independent of *farl-11*.

#### ***farl-11* promotes *glp-1* activity**

In *C. elegans*, GLP-1/Notch signaling maintains GSCs in the distal germline. In mutants lacking *glp-1* activity, GSCs are lost due to premature meiotic differentiation. As mentioned above, *farl-11(kp35)* germlines have fewer germ cells than the wild type. In addition, like the *glp-1* null mutants, the *farl-11 puf-8* double-mutant adults lack GSCs and express the meiotic marker HIM-3 even in the distal-most germ cells (Fig. 2). These observations prompted us to investigate the genetic interaction, if any, between *farl-11* and *glp-1*. For this, we generated a double-mutant strain

carrying *farl-11(kp35)* and *glp-1(ar202)*, which is a weak gain-of-function (*gf*) temperature-sensitive allele (Pepper et al., 2003). *glp-1(ar202)* worms are fertile at 15°C but display germline defects, primarily mitotic proliferation of germ cells at the proximal gonad (Pro phenotype) and extension of the distal mitotic region, when grown at 25°C (Pepper et al., 2003). Even at 15°C, the distal mitotic region of *glp-1(ar202)* germlines is more extended than in the wild type (Fig. 8A). At 25°C, the germline defects of *farl-11(kp35); glp-1(ar202)* worms were similar to those of the *glp-1(ar202)* single mutant (data not shown). However, at 15°C the distal mitotic region of *farl-11(kp35); glp-1(ar202)* germlines was significantly shorter than that of *glp-1(ar202)* germlines (Fig. 8A,B).

Next, we tested the effect of *farl-11(kp35)* on the phenotype of *glp-1(q231)*, which is a temperature-sensitive loss-of-function (*lf*) allele. Adults homozygous for *glp-1(q231)* are sterile and lack GSCs when grown at 25°C, but are fertile and possess GSCs when maintained at 15°C (Austin and Kimble, 1987). By contrast, *farl-11(kp35); glp-1(q231)* adults had fewer (77%,  $n=101$ ) or no (23%,  $n=101$ ) GSCs even when continuously maintained at 15°C (Fig. 8C). Thus, *farl-11(kp35)* suppresses the gain-of-function and enhances the loss-of-function phenotypes of *glp-1*. However, unlike

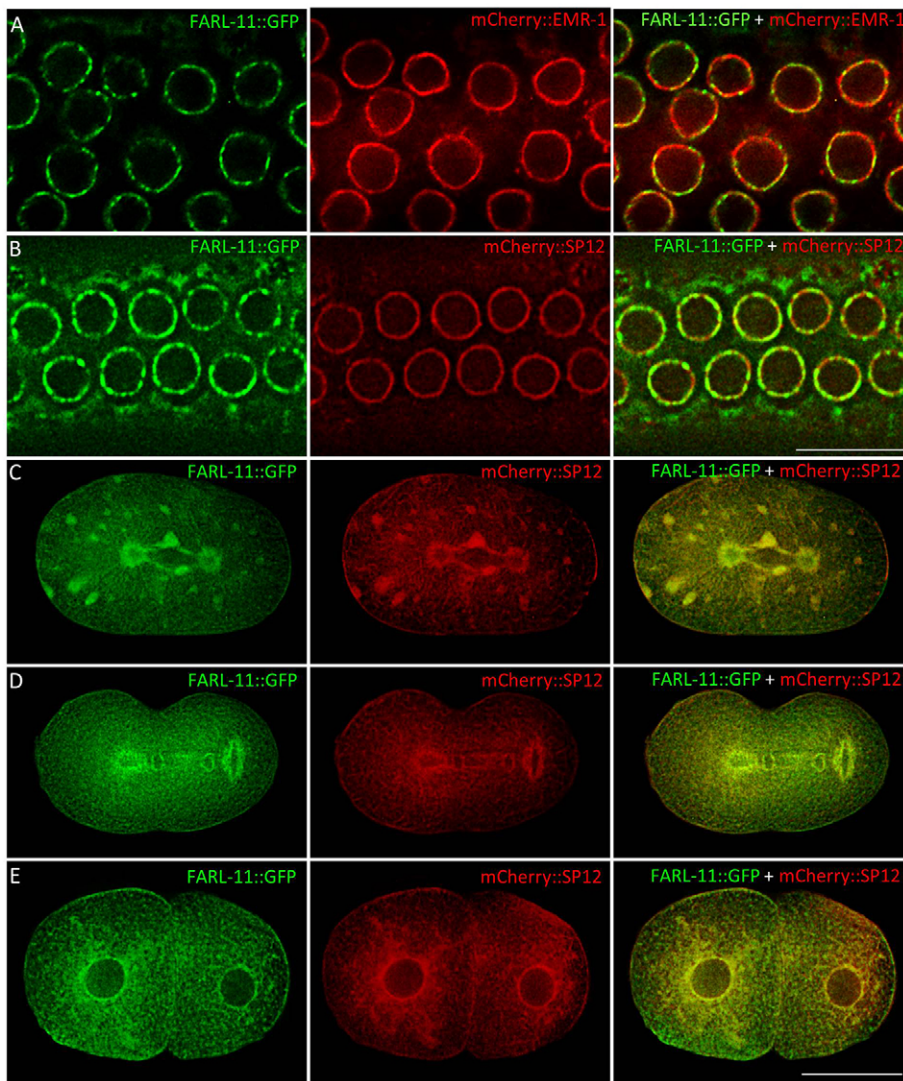


**Fig. 6. FARL-11::GFP localizes on ER.** (A) A section of the germline showing a few germ nuclei that express FARL-11::GFP and the NE marker mCherry::EMR-1 (strain IT867). (B) Expression patterns of FARL-11::GFP and the ER marker mCherry::SP12 (strain IT939) in the germline. FARL-11::GFP and mCherry::SP12 colocalize on NE. (C-E) FARL-11::GFP and mCherry::SP12 show strong colocalization throughout the cell division cycle in embryos; (C) metaphase, (D) telophase, (E) interphase. Scale bars: 20  $\mu$ m.

*glp-1* null mutants, which form sperm, no sperm was present in the *farl-11(kp35); glp-1(q231)* germlines, presumably owing to meiotic defects (see above and Fig. 1). Furthermore, the oocytes in *farl-11(kp35)* worms were larger than those of the wild type (Fig. 8D), a phenotype strikingly similar to that observed in *glp-1(lf)* worms (Nadarajan et al., 2009). Together, the above data reveal that *farl-11* promotes *glp-1* activity.

#### ***farl-11* is essential for GLP-1 localization**

GLP-1 is a transmembrane receptor of the LIN-12/Notch family. Since such transmembrane proteins are synthesized on ER, the structural and functional integrity of the ER is likely to be crucial for membrane localization of GLP-1 and, consequently, for *glp-1* activity. Therefore, in *farl-11(kp35)* germlines, it is possible that the altered ER morphology compromises normal GLP-1 localization. To test this, we immunostained the germlines with anti-GLP-1 antibodies and compared the distribution patterns of GLP-1 among wild-type, *farl-11(kp35)*, *farl-11(kp35) puf-8(zh17)* and *farl-11(kp35) farl-11(RNAi)* germlines. As shown in Fig. 9A, a honeycomb-like pattern of staining, reflecting the membrane localization of GLP-1, was readily observable in wild-type and *farl-11(kp35)* germlines, although the *farl-11(kp35)* germ cells appeared larger, especially in the proximal part. By contrast, the honeycomb pattern was completely absent in *farl-11(kp35) puf-8*

(*zh17*) and *farl-11(kp35) farl-11(RNAi)* germlines. Instead, GLP-1 formed aggregates in the central lumen at the distalmost germline. No membrane-localized GLP-1 could be detected in more proximal germ cells.

A GFP fusion of the transmembrane yolk receptor RME-2 (Grant and Hirsh, 1999), which was not detectable in the cytoplasm of wild-type oocytes, accumulated around the nucleus in some of the FARL-11-deficient oocytes (Fig. S8). However, the localization of other membrane proteins, such as the syntaxin SYN-4 and phospholipase C, which do not depend on the ER for synthesis and transport, were unaffected (Fig. S8). Thus, the localization defects of GLP-1 in the *farl-11* mutant most likely result from defects in the ER-dependent synthesis and/or transport of GLP-1, and not from defects in plasma membrane structure.

#### **The effect of *farl-11* on germ cell proliferation is mediated through GLP-1**

As mentioned in the Introduction, GLP-1 promotes germ cell proliferation primarily by suppressing the meiotic promoters *gld-1* and *gld-2*; in the absence of *gld-1* and *gld-2* activities, *glp-1* is not required for germ cell proliferation (Kadyk and Kimble, 1998). Based on this, we predicted that the mitotic proliferation of germ cells would be restored in *farl-11(kp35) puf-8(zh17)* worms upon depletion of GLD-1 and GLD-2 if FARL-11 promotes germ cell



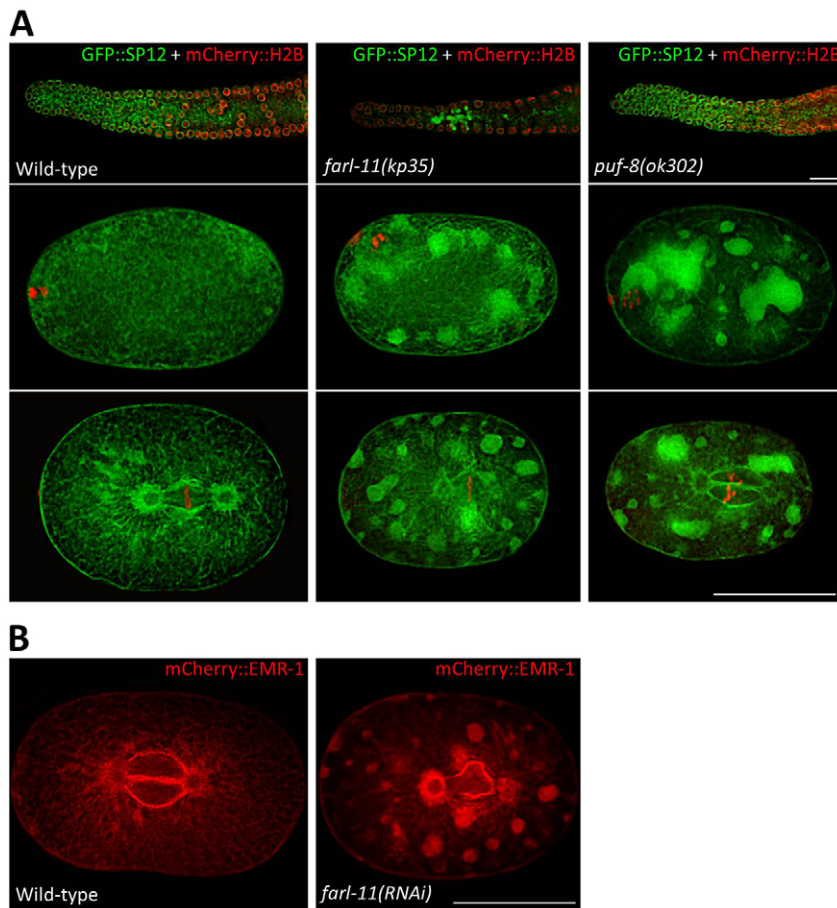


**Fig. 7. *farl-11* and *puf-8* mutations alter ER morphology.** (A) Germlines and embryos expressing the ER marker GFP::SP12 and the chromatin marker mCherry::H2B (strain IT938). Only the distal part of the germline is shown. ER is seen evenly distributed in the lumen of wild-type and *puf-8* mutant germlines; by contrast, it forms large clumps in the *farl-11* mutant (top row). Similarly, ER forms numerous large patches in the cytoplasm at both meiotic (middle row) and mitotic (bottom row) metaphases in *farl-11* as well as *puf-8* mutant embryos. Similar large ER patches were seen in worms depleted of CASH-1, another FAR complex protein (see Fig. S4). (B) Cytoplasmic patches are observed with the NE marker mCherry::EMR-1 in the FARL-11-depleted embryo (strain IT305). See Movies 1–3 for a comparison of ER dynamics in wild-type, *farl-11(kp35)* and *puf-8(ok302)* worms, respectively, during the first cleavage. Scale bars: 20  $\mu$ m.

proliferation by facilitating GLP-1 localization. As shown in Fig. 9B, germ cell proliferation was indeed restored in all *farl-11 puf-8* double-mutant germlines depleted of GLD-1 and GLD-2 by RNAi ( $n=110$ ). Thus, like GLP-1, FARL-11 is not required for germ cell proliferation when meiotic entry is blocked. We conclude that FARL-11 contributes to GSC maintenance by promoting the membrane localization of GLP-1.

## DISCUSSION

Although the FAR complex has been shown to be anchored on ER in yeast, whether this complex contributes to ER dynamics or function was not known (Pracheil and Liu, 2013). Our work reveals that *C. elegans* FARL-11, which is an ortholog of yeast FAR11, is present on ER and is essential for normal ER dynamics. In addition, FARL-11 appears to be important for ER function as well: the membrane localization of GLP-1/Notch receptor, which mediates niche-GSC interaction, is significantly compromised in the absence of FARL-11. Furthermore, our results indicate that PUF-8, a conserved translational regulator in the germline, promotes FARL-11 expression post-transcriptionally. Thus, the results presented here identify an important link among translational control, ER dynamics and niche-GSC signaling.

The *kp35* allele of *farl-11* was isolated as an enhancer of the *puf-8* mutant phenotype. Two important observations, when taken together, suggest a model that explains the genetic interaction between *farl-11* and *puf-8*. First, although *farl-11(kp35)* worms were not sterile, they became sterile when depleted of the mutant FARL-11 protein by RNAi. Further, defects in *farl-11(kp35) puf-8(zh17)* and *farl-11(kp35) farl-11(RNAi)* germlines were similar:

both lacked membrane-localized GLP-1. Second, our results strongly suggest that PUF-8 promotes FARL-11 expression in the germline. Thus, it is possible that the *kp35* mutation weakens FARL-11 activity to some extent, but not sufficiently to compromise its germline function as long as its expression is not disrupted. However, in *farl-11(kp35) puf-8(zh17)* worms, not only will FARL-11 activity be weaker due to the *kp35* mutation, but also its expression will be diminished due to the lack of PUF-8 activity. Thus, the double-mutant phenotype might reflect the reduced expression of a partially active FARL-11. Nonetheless, in the absence of a null allele of *farl-11*, and given that PUF-8 controls the expression of several other genes in the germline, we cannot rule out the possibility that the double-mutant phenotype might result from the combined effect of reduced *farl-11* activity and the misexpression of other factor(s) controlled by *puf-8*.

Several lines of evidence indicate that *farl-11* controls germ cell proliferation, at least in part, by promoting *glp-1* activity. First, germ cells prematurely enter meiosis in the *farl-11 puf-8* double mutant and *farl-11(kp35)* oocytes are larger than those of the wild type – phenotypes that are strikingly similar to those of *glp-1(lf)* and *glp-1(rf)*, respectively (Austin and Kimble, 1987; Nadarajan et al., 2009). Second, *farl-11(kp35)* enhances the *glp-1(rf)* phenotype and suppresses the *glp-1(gf)* phenotype. Third, membrane localization of GLP-1 is severely compromised in *farl-11(-)* [*farl-11(kp35) puf-8(-)* or *farl-11(kp35) farl-11(RNAi)*] germ cells. Finally, *farl-11* promotes proliferation by preventing meiotic entry, which resembles the main function of *glp-1* in the germline (Kadyk and Kimble, 1998). How does *farl-11* promote *glp-1* activity? Since GLP-1 is a transmembrane receptor protein, the functional integrity



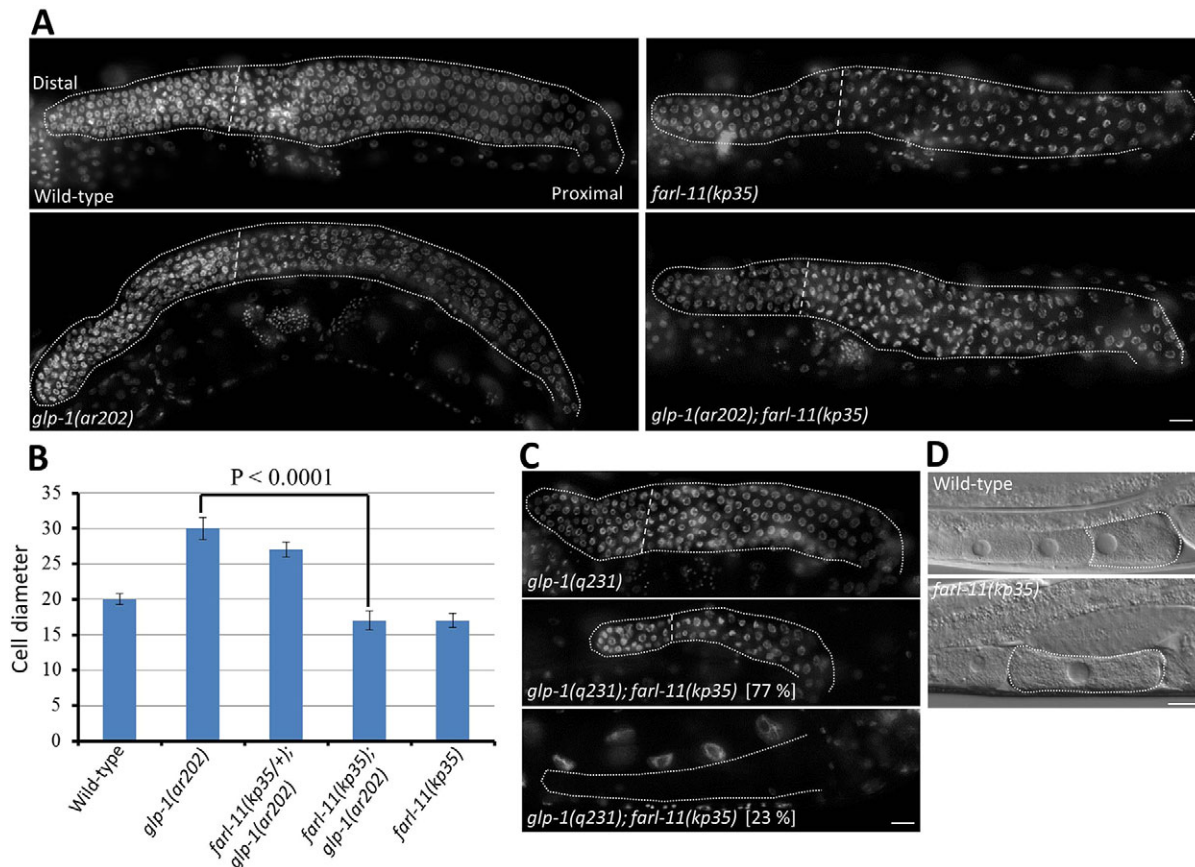


**Fig. 8. The *farl-1(kp35)* mutation suppresses the gain-of-function phenotypes and enhances the loss-of-function phenotypes of *glp-1*.** (A,C) Germlines from 2-day adult hermaphrodites of the indicated genotypes stained with DAPI. The vertical dashed lines mark the boundary between the mitotic and transition zones. Whereas the mitotic zone extends in worms homozygous for *glp-1(ar202)* (strain GC833), it is significantly shorter in *glp-1(ar202); farl-1(kp35)* worms (strain IT871). (B) Quantitation of the results shown in A. The number of germ nuclei in a single row between the distal end and the beginning of the transition zone was counted to determine the length of the distal mitotic zone in cell diameters. Error bars indicate s.d.  $P < 0.0001$  [Student's *t*-test for *glp-1(ar202)* versus *farl-1(kp35); glp-1(ar202)*]. (C) Worms homozygous for *q231* (strain JK509), a weak loss-of-function *glp-1* allele at 15°C, have smaller germlines than the wild type, which are further reduced in the *glp-1(q231); farl-1(kp35)* (strain IT870) double mutant (middle, 77%); in some double-mutant germlines, no germ cells could be observed (bottom, 23%). All genotypes shown in A and C were grown at 15°C. (D) DIC/Nomarski images of wild-type and *farl-1(kp35)* oocytes. The proximalmost oocyte is outlined. The *farl-1* mutant oocyte is ~1.5-times larger than that of the wild type.  $n=11$  oocytes;  $P < 0.0001$  [Student's *t*-test for *farl-1(kp35)* versus wild type]. A similar phenotype is caused by reduction-of-function (rf) *glp-1* alleles (Nadarajan et al., 2009). Scale bars: 20  $\mu$ m.

of ER will be crucial for its synthesis and transport to the cell membrane. Thus, one possibility is that the ER defects observed in *farl-1(-)* germlines disrupt GLP-1 synthesis and/or transport to the membrane. FARL-11 orthologs in other organisms control the phosphorylation status of certain proteins by regulating the activity of PP2A phosphatase (see below). So, an alternative possibility is that FARL-11 modulates the GLP-1/Notch signaling pathway by regulating the phosphorylation status of a component(s) of this pathway. In any case, ER defects or a change in PP2A activity will have consequences for the activity of several factors. Therefore, *farl-1* is likely to influence the functions of many other factors besides *glp-1*. Consistently, although *farl-1 puf-8* double-mutant germ cells prematurely enter meiosis, they fail to complete meiosis, which is distinct from the *glp-1(lf)* phenotype.

How does FARL-11 contribute to ER integrity? Although we do not yet have a definitive answer to this question, we can propose certain models based on published data and our current results. In yeast, FAR11 promotes PP2A phosphatase activity and antagonizes TOR signaling (Pracheil et al., 2012). FAR11 and PP2A are components of the FAR complex anchored on the ER (Pracheil and Liu, 2013). The *Drosophila* ortholog of FAR11 is also part of the fly STRIPAK PP2A complex, which negatively regulates Hippo

signaling by reducing the levels of phosphorylated Hippo (Ribeiro et al., 2010). STRIP1/2, the human counterparts of FAR11, control cell contractility through negative regulation of the MST3 (STK24) and MST4 (STK26) kinases (Madsen et al., 2015). Thus, positive regulation of PP2A activity appears to be a conserved function of FAR11/STRIP; the *C. elegans* FARL-11 might also regulate PP2A activity.

How does a possible regulation of PP2A link FARL-11 with ER dynamics? ER associates with microtubules, and both dynein and kinesin motor proteins are essential for the morphological changes in ER during the cell cycle (Du et al., 2004). The dynein-dependent ER movement appears to be controlled by phosphorylation (Allan, 1995). Thus, one possibility is that ER-localized FARL-11 controls dynein-dependent ER movement by regulating dynein phosphorylation. Significantly, reduction of *farl-11* expression by RNAi has been shown to suppress the phenotype of a *C. elegans* dynein heavy chain mutant, suggesting that FARL-11 might indeed regulate dynein function (O'Rourke et al., 2007).

In *C. elegans* embryos, homotypic membrane fusion is essential for cell cycle-dependent ER dynamics. Depletion of proteins that promote homotypic membrane fusion, such as the Cdc48/p97 AAA-ATPase ortholog CDC-48.3 or the heat shock protein BIP

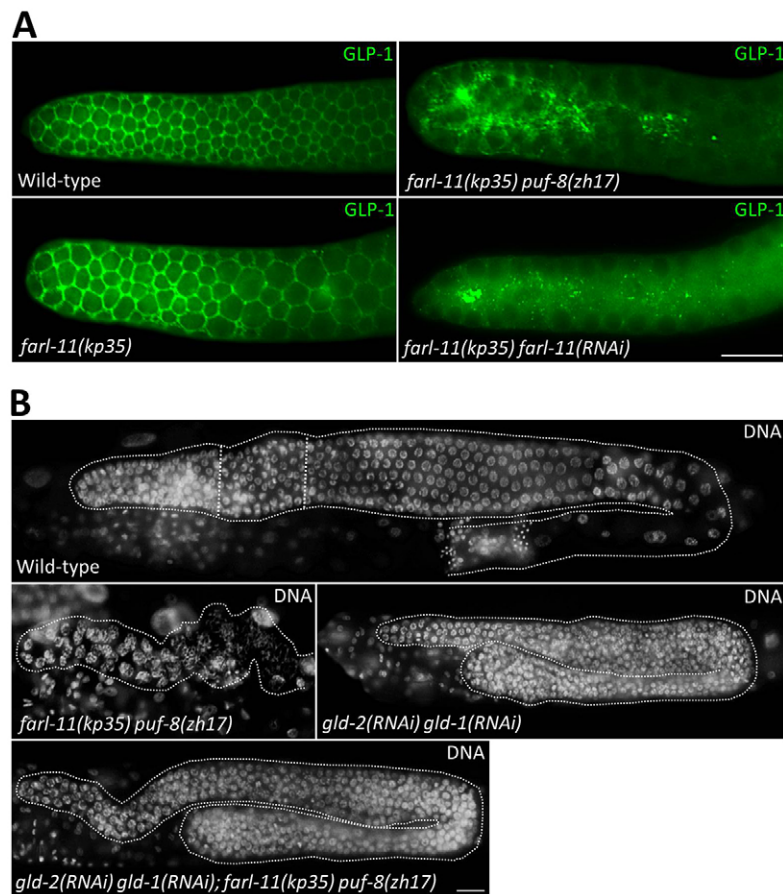


**Fig. 9. FARL-11 promotes GLP-1 activity by facilitating its membrane localization.** (A) Dissected gonads immunostained for GLP-1. Only the distal region is shown. A honeycomb-like staining pattern characteristic of germ cell membranes is seen in the wild-type and *farl-11(kp35)* (strain IT719) germlines. By contrast, the membrane localization of GLP-1 is absent, at least in more proximal germ cells, in the *farl-11 puf-8* (strain 73) double-mutant and *farl-11(kp35) farl-11(RNAi)* (strain IT719) germlines. Instead, GLP-1 forms aggregates in the lumen. (B) DAPI-stained germlines in intact worms of the indicated genotypes. Proliferating germ cells are restored in the *farl-11 puf-8* (strain IT73) double mutant upon depletion of the meiotic promoters GLD-1 and GLD-2, which is strikingly similar to that observed in *glp-1(-)* worms (Kadyk and Kimble, 1998). The vertical dashed lines in the wild-type germline mark the boundaries between the mitotic, transition and pachytene zones; only mitotic germ cells are present in *gld-2(RNAi) gld-1(RNAi)* and *gld-2(RNAi) gld-1(RNAi); farl-11(kp35) puf-8(RNAi)* germlines. Scale bars: 20  $\mu$ m.

ortholog HSP-4, leads to the accumulation of large ER patches, which are strikingly similar to those we observed in *farl-11(kp35)* embryos (Poteryaev et al., 2005). Cdc48/p97 and BiP have been shown to be regulated by phosphorylation/dephosphorylation in other organisms (Diaz-Troya et al., 2011; Hendershot et al., 1988; Lavoie et al., 2000; Li et al., 2008). In the unicellular green alga *Chlamydomonas reinhardtii*, BiP phosphorylation is regulated by the TOR pathway, which, as mentioned above, is regulated by the FARL1-PP2A complex in yeast (Crespo, 2012). Therefore, it is possible that FARL-11 might play a role in homotypic membrane fusion, and consequently in ER dynamics, by controlling the phosphorylation status of CDC-48.3 or HSP-4, either directly or by regulating the TOR pathway.

A third alternative model is that PUF-8 and FARL-11 contribute to ER dynamics by regulating the ER stress response. Since PUF-8 suppresses the translation of several germline transcripts, the corresponding protein products will be misexpressed in the absence of PUF-8, and some of them possibly accumulate in the ER. If FARL-11 controls the phosphorylation status of HSP-4, which is the *C. elegans* ortholog of BiP (see above), then its absence is likely to compromise the ER stress response, as BiP plays a major role in protein folding as well as in the degradation of unfolded proteins (Otero et al., 2010). Thus, the alterations in ER dynamics observed in the *farl-11 puf-8* double mutant might have resulted from the simultaneous accumulation of misexpressed proteins and the failure of the ER stress response. Establishing whether FARL-11 indeed controls PP2A, or any other protein phosphatase, in *C. elegans* and the identification of downstream targets will help in distinguishing among these alternative models.

## MATERIALS AND METHODS

### *C. elegans* strains

Genotypes of strains used in this study are provided in Table S1. Strains were maintained at 20°C as described (Brenner, 1974), except the strains carrying the temperature-sensitive *glp-1* alleles *ar202* and *q231*, which were maintained at 15°C. Generation of double-mutant strains and the introduction of transgenes into different genetic backgrounds were performed using standard genetic techniques. Genome sequencing and analysis of the sequence data for the IT73 strain were performed by the Genome Technology Access Center in the Department of Genetics at Washington University School of Medicine. During routine strain maintenance, the presence of the *kp35* allele was detected by PCR using primers KS3949 and KS3950 (Table S2). Genetic mapping of the *kp35* mutation and construction of the various transgenes used in this study are described in the supplementary Materials and Methods.

### Immunostaining and fluorescence microscopy

Gonads were dissected and fixed for staining of DNA with DAPI as described (Francis et al., 1995). Immunostaining with anti-HIM-3, anti-PH3 and anti-GLP antibodies was performed according to Ariz et al. (2009). Incubation with primary and secondary antibodies was carried out as described previously (Subramaniam and Seydoux, 1999). Primary antibodies for GLP-1 and PH3 were used at 1:50 and 1:1000, respectively; for HIM-3, undiluted, affinity-purified polyclonal antibodies were used.

Fluorescence images of immunostained gonads were mounted in Vectashield (Vector Laboratories) and examined using a Zeiss Axio Imager M2 fluorescence microscope. Germlines and embryos expressing GFP and mCherry reporter fusions were also examined similarly. All images presented here were acquired using a Zeiss Axiocam HRm CCD camera and are representative of at least 50 specimens per experiment, and the experiments were repeated at least four times. Images shown in Figs 5–7 and Figs S6, S7 were obtained by deconvolving the original images using the Deconvolution module of Axiovision software (Zeiss).



**EMSA**

EMSAs were carried out as described previously (Jadhav et al., 2008). The DNA fragment corresponding to the *farl-11* 3' UTR was PCR amplified using primers KS3965 and KS4252 (Table S2) and cloned into pSV2 vector using the T/A cloning procedure (Mainpal et al., 2011). Orientation of the insert was determined by PCR using the vector-specific primer KS2808 and the insert-specific primer KS4252. The KS2808-KS4252 PCR product served as the template for *in vitro* transcription of the *farl-11* 3' UTR RNA used in EMSAs.

**Co-immunoprecipitation and RT-PCR**

The PUF-8::9xHA::GFP fusion protein was immunoprecipitated from lysates prepared from strain IT722 using the procedure described by Vaid et al. (2013). Co-immunoprecipitation of *farl-11* mRNA was determined by RT-PCR using primers KS3965 and KS4252. As a negative control, an RT-PCR product corresponding to *pie-1* mRNA was amplified using primers KS1102 and KS2495 (Table S2).

**Acknowledgements**

We thank Anne Helsing and Judith Kimble for the anti-GLP-1 antibody; Anne Spang for *C. elegans* strain SP12 (GFP::SP12); Orna Cohen-Fix for strain OCF15 (mCherry::SP12); and the National BioResource Project, Japan, for the *tm6233* allele. Several of the *C. elegans* strains used in this study were provided by the Caenorhabditis Genetics Center, which is funded by the National Institutes of Health Office of Research Infrastructure Programs [P40 OD010440].

**Competing interests**

The authors declare no competing or financial interests.

**Author contributions**

K.P., R.M. and K.S. designed the research; K.P. and K.S. mapped the *kp35* allele, performed preliminary phenotypic analysis and 3' reporter fusion experiments; R.M. determined the FARL-11 expression pattern, and performed the EMSA, Co-IP and the genetic interaction studies; K.S. wrote the manuscript. All authors approved the final version of the manuscript.

**Funding**

Research in the K.S. laboratory is supported by grants from the Indian Council of Agricultural Research through the National Fund Scheme; and by the Department of Biotechnology and the Department of Science and Technology, Ministry of Science and Technology, Government of India.

**Supplementary information**

Supplementary information available online at <http://dev.biologists.org/lookup/doi/10.1242/dev.134056.supplemental>

**References**

- Allan, V. (1995). Protein phosphatase 1 regulates the cytoplasmic dynein-driven formation of endoplasmic reticulum networks *in vitro*. *J. Cell Biol.* **128**, 879-891.
- Ariz, M., Mainpal, R. and Subramaniam, K. (2009). *C. elegans* RNA-binding proteins PUF-8 and MEX-3 function redundantly to promote germline stem cell mitosis. *Dev. Biol.* **326**, 295-304.
- Audhya, A., Desai, A. and Oegema, K. (2007). A role for Rab5 in structuring the endoplasmic reticulum. *J. Cell Biol.* **178**, 43-56.
- Austin, J. and Kimble, J. (1987). *glp-1* is required in the germ line for regulation of the decision between mitosis and meiosis in *C. elegans*. *Cell* **51**, 589-599.
- Bachorik, J. L. and Kimble, J. (2005). Redundant control of the Caenorhabditis elegans sperm/oocyte switch by PUF-8 and FBF-1, two distinct PUF RNA-binding proteins. *Proc. Natl. Acad. Sci. USA* **102**, 10893-10897.
- Bonner, M. K., Han, B. H. and Skop, A. (2013). Profiling of the mammalian mitotic spindle proteome reveals an ER protein, OSTD-1, as being necessary for cell division and ER morphology. *PLoS ONE* **8**, e77051.
- Brenner, S. (1974). The genetics of Caenorhabditis elegans. *Genetics* **77**, 71-94.
- Ciosk, R., DePalma, M. and Priess, J. R. (2004). ATX-2, the *C. elegans* ortholog of ataxin 2, functions in translational regulation in the germline. *Development* **131**, 4831-4841.
- Crespo, J. L. (2012). BiP links TOR signaling to ER stress in Chlamydomonas. *Plant Signal. Behav.* **7**, 273-275.
- Crittenden, S. L., Bernstein, D. S., Bachorik, J. L., Thompson, B. E., Gallegos, M., Petcherski, A. G., Moulder, G., Barstead, R., Wickens, M. and Kimble, J. (2002). A conserved RNA-binding protein controls germline stem cells in Caenorhabditis elegans. *Nature* **417**, 660-663.
- D'Agostino, I., Merritt, C., Chen, P.-L., Seydoux, G. and Subramaniam, K. (2006). Translational repression restricts expression of the *C. elegans* Nanos homolog NOS-2 to the embryonic germline. *Dev. Biol.* **292**, 244-252.
- Diaz-Troya, S., Perez-Perez, M. E., Perez-Martin, M., Moes, S., Jenó, P., Florencio, F. J. and Crespo, J. L. (2011). Inhibition of protein synthesis by TOR inactivation revealed a conserved regulatory mechanism of the BiP chaperone in Chlamydomonas. *Plant Physiol.* **157**, 730-741.
- Du, Y., Ferro-Novick, S. and Novick, P. (2004). Dynamics and inheritance of the endoplasmic reticulum. *J. Cell Sci.* **117**, 2871-2878.
- Forbes, A. and Lehmann, R. (1998). Nanos and Pumilio have critical roles in the development and function of Drosophila germline stem cells. *Development* **125**, 679-690.
- Francis, R., Barton, M. K., Kimble, J. and Schedl, T. (1995). *gld-1*, a tumor suppressor gene required for oocyte development in Caenorhabditis elegans. *Genetics* **139**, 579-606.
- Grant, B. and Hirsh, D. (1999). Receptor-mediated endocytosis in the Caenorhabditis elegans oocyte. *Mol. Biol. Cell* **10**, 4311-4326.
- Hendershot, L. M., Ting, J. and Lee, A. S. (1988). Identity of the immunoglobulin heavy-chain-binding protein with the 78,000-dalton glucose-regulated protein and the role of posttranslational modifications in its binding function. *Mol. Cell. Biol.* **8**, 4250-4256.
- Hoozemans, J. J. M., Stieler, J., van Haastert, E. S., Veerhuis, R., Rozemuller, A. J. M., Baas, F., Eikelenboom, P., Arendt, T. and Scheper, W. (2006). The unfolded protein response affects neuronal cell cycle protein expression: implications for Alzheimer's disease pathogenesis. *Exp. Gerontol.* **41**, 380-386.
- Hwang, J. and Pallas, D. C. (2014). STRIPAK complexes: structure, biological function, and involvement in human diseases. *Int. J. Biochem. Cell Biol.* **47**, 118-148.
- Jadhav, S., Rana, M. and Subramaniam, K. (2008). Multiple maternal proteins coordinate to restrict the translation of *C. elegans* nanos-2 to primordial germ cells. *Development* **135**, 1803-1812.
- Jamora, C., Dennert, G. and Lee, A. S. (1996). Inhibition of tumor progression by suppression of stress protein GRP78/BiP induction in fibrosarcoma B/C10ME. *Proc. Natl. Acad. Sci. USA* **93**, 7690-7694.
- Joseph-Strauss, D., Gorjanacz, M., Santarella-Mellwig, R., Voronina, E., Audhya, A. and Cohen-Fix, O. (2012). Sm protein down-regulation leads to defects in nuclear pore complex disassembly and distribution in *C. elegans* embryos. *Dev. Biol.* **365**, 445-457.
- Kadyk, L. C. and Kimble, J. (1998). Genetic regulation of entry into meiosis in Caenorhabditis elegans. *Development* **125**, 1803-1813.
- Kemp, H. A. and Sprague, G. F., Jr. (2003). Far3 and five interacting proteins prevent premature recovery from pheromone arrest in the budding yeast *Saccharomyces cerevisiae*. *Mol. Cell. Biol.* **23**, 1750-1763.
- Lant, B., Yu, B., Goudreaux, M., Holmyard, D., Knight, J. D. R., Xu, P., Zhao, L., Chin, K., Wallace, E., Zhen, M. et al. (2015). CCM-3/STRIPAK promotes seamless tube extension through endocytic recycling. *Nat. Commun.* **6**, 6449.
- Lavoie, C., Chevret, E., Roy, L., Tonks, N. K., Fazel, A., Posner, B. I., Paiement, J. and Bergeron, J. J. M. (2000). Tyrosine phosphorylation of p97 regulates transitional endoplasmic reticulum assembly *in vitro*. *Proc. Natl. Acad. Sci. USA* **97**, 13637-13642.
- Lehmann, R. and Nusslein-Volhard, C. (1987). Involvement of the *pumilio* gene in the transport of an abdominal signal in the *Drosophila* embryo. *Nature* **329**, 167-170.
- Li, G., Zhao, G., Schindelin, H. and Lennarz, W. J. (2008). Tyrosine phosphorylation of ATPase p97 regulates its activity during ERAD. *Biochem. Biophys. Res. Commun.* **375**, 247-251.
- Madsen, C. D., Hooper, S., Tozluoglu, M., Bruckbauer, A., Fletcher, G., Erler, J. T., Bates, P. A., Thompson, B. and Sahai, E. (2015). STRIPAK components determine mode of cancer cell migration and metastasis. *Nat. Cell Biol.* **17**, 68-80.
- Mainpal, R., Priti, A. and Subramaniam, K. (2011). PUF-8 suppresses the somatic transcription factor PAL-1 expression in *C. elegans* germline stem cells. *Dev. Biol.* **360**, 195-207.
- Nadarajan, S., Govindan, J. A., McGovern, M., Hubbard, E. J. A. and Greenstein, D. (2009). MSP and GLP-1/Notch signaling coordinately regulate actomyosin-dependent cytoplasmic streaming and oocyte growth in *C. elegans*. *Development* **136**, 2223-2234.
- O'Rourke, S. M., Dorfman, M. D., Carter, J. C. and Bowerman, B. (2007). Dynein modifiers in *C. elegans*: light chains suppress conditional heavy chain mutants. *PLoS Genet.* **3**, e128.
- Otero, J. H., Lizak, B. and Hendershot, L. M. (2010). Life and death of a BiP substrate. *Semin. Cell Dev. Biol.* **21**, 472-478.
- Pepper, A. S., Killian, D. J. and Hubbard, E. J. (2003). Genetic analysis of Caenorhabditis elegans *glp-1* mutants suggests receptor interaction or competition. *Genetics* **163**, 115-132.
- Poteryaev, D., Squirrel, J. M., Campbell, J. M., White, J. G. and Spang, A. (2005). Involvement of the actin cytoskeleton and homotypic membrane fusion in ER dynamics in Caenorhabditis elegans. *Mol. Biol. Cell* **16**, 2139-2153.
- Pracheil, T. and Liu, Z. (2013). Tiered assembly of the yeast Far3-7-8-9-10-11 complex at the endoplasmic reticulum. *J. Biol. Chem.* **288**, 16986-16997.

- Pracheil, T., Thornton, J. and Liu, Z.** (2012). TORC2 signaling is antagonized by protein phosphatase 2A and the Far complex in *Saccharomyces cerevisiae*. *Genetics* **190**, 1325-1339.
- Priti, A. and Subramaniam, K.** (2015). PUF-8 functions redundantly with GLD-1 to promote the meiotic progression of spermatocytes in *Caenorhabditis elegans*. *G3 (Bethesda)* **5**, 1675-1684.
- Puhka, M., Vihinen, H., Joensuu, M. and Jokitalo, E.** (2007). Endoplasmic reticulum remains continuous and undergoes sheet-to-tubule transformation during cell division in mammalian cells. *J. Cell Biol.* **179**, 895-909.
- Racher, H. and Hansen, D.** (2012). PUF-8, a Pumilio homolog, inhibits the proliferative fate in the *Caenorhabditis elegans* germline. *G3 (Bethesda)* **2**, 1197-1205.
- Ribeiro, P. S., Josue, F., Wepf, A., Wehr, M. C., Rinner, O., Kelly, G., Tapon, N. and Gstaiger, M.** (2010). Combined functional genomic and proteomic approaches identify a PP2A complex as a negative regulator of Hippo signaling. *Mol. Cell* **39**, 521-534.
- Sanchez-Alvarez, M., Finger, F., Arias-Garcia, M. d. M., Bousgouni, V., Pascual-Vargas, P. and Bakal, C.** (2014). Signaling networks converge on TORC1-SREBP activity to promote endoplasmic reticulum homeostasis. *PLoS ONE* **9**, e101164.
- Scheuner, D., Vander Mierde, D., Song, B., Flamez, D., Creemers, J. W. M., Tsukamoto, K., Ribick, M., Schuit, F. C. and Kaufman, R. J.** (2005). Control of mRNA translation preserves endoplasmic reticulum function in beta cells and maintains glucose homeostasis. *Nat. Med.* **11**, 757-764.
- Schlaitz, A.-L., Thompson, J., Wong, C. C. L., Yates, J. R., III and Heald, R.** (2013). REEP3/4 ensure endoplasmic reticulum clearance from metaphase chromatin and proper nuclear envelope architecture. *Dev. Cell* **26**, 315-323.
- Shibata, Y., Voeltz, G. K. and Rapoport, T. A.** (2006). Rough sheets and smooth tubules. *Cell* **126**, 435-439.
- Souza, G. M., da Silva, A. M. and Kuspa, A.** (1999). Starvation promotes *Dictyostelium* development by relieving PufA inhibition of PKA translation through the YakA kinase pathway. *Development* **126**, 3263-3274.
- Subramaniam, K. and Seydoux, G.** (1999). *nos-1* and *nos-2*, two genes related to *Drosophila nanos*, regulate primordial germ cell development and survival in *Caenorhabditis elegans*. *Development* **126**, 4861-4871.
- Subramaniam, K. and Seydoux, G.** (2003). Dedifferentiation of primary spermatocytes into germ cell tumors in *C. elegans* lacking the pumilio-like protein PUF-8. *Curr. Biol.* **13**, 134-139.
- Vaid, S., Ariz, M., Chaturvedi, A., Kumar, G. A. and Subramaniam, K.** (2013). PUF-8 negatively regulates RAS/MAPK signalling to promote differentiation of *C. elegans* germ cells. *Development* **140**, 1645-1654.
- Walser, C. B., Battu, G., Hoier, E. F. and Hajnal, A.** (2006). Distinct roles of the Pumilio and FBF translational repressors during *C. elegans* vulval development. *Development* **133**, 3461-3471.
- Wang, S., Romano, F. B., Field, C. M., Mitchison, T. J. and Rapoport, T. A.** (2013). Multiple mechanisms determine ER network morphology during the cell cycle in *Xenopus* egg extracts. *J. Cell Biol.* **203**, 801-814.
- Xu, E. Y., Chang, R., Salmon, N. A. and Reijo Pera, R. A.** (2007). A gene trap mutation of a murine homolog of the *Drosophila* stem cell factor Pumilio results in smaller testes but does not affect litter size or fertility. *Mol. Reprod. Dev.* **74**, 912-921.
- Zetka, M. C., Kawasaki, I., Strome, S. and Muller, F.** (1999). Synapsis and chiasma formation in *Caenorhabditis elegans* require HIM-3, a meiotic chromosome core component that functions in chromosome segregation. *Genes Dev.* **13**, 2258-2270.
- Zhang, B., Gallegos, M., Puoti, A., Durkin, E., Fields, S., Kimble, J. and Wickens, M. P.** (1997). A conserved RNA-binding protein that regulates sexual fates in the *C. elegans* hermaphrodite germ line. *Nature* **390**, 477-484.



## SUPPLEMENTARY METHODS

### Genetic mapping of *kp35*

Two 3-factor crosses were performed. In the first cross, hermaphrodites homozygous for *bli-2(e768) puf-8(zh17) rol-6(e187)* were mated with *kp35 puf-8(zh17) unc-4(e120) / mC6g* males. Among the progeny, 22 out of 29 non-blister roller worms (recombinants) were fertile. In the second cross, hermaphrodites homozygous for *unc-104(e1265) puf-8(zh17) rol-6(e187)* were mated with *kp35 puf-8(zh17) unc-4(e120) / mC6g* males. Two out of 78 roller progeny (recombinants) from this cross were fertile. These results placed *kp35* on the right of, but very close to, *unc-104* i.e., between 0.2 and 0.5 map position on chromosome II.

A comparison of the mutant and wild-type genome sequences revealed three G-to-A substitutions in the above genetic interval. All three were missense mutations leading to amino acid changes in HIM-14 (proline to leucine at position 362), ADA-2 (glycine to arginine at 98) and FARL-11 (serine to leucine at 169) (Fig. S1 and data not shown). The deletion allele *ok230*, which disrupts *him-14* function, did not enhance the *puf-8* phenotype. In addition, separation of the newly-isolated *him-14* point mutation from *puf-8(zh17)* did not suppress the *puf-8(zh17) kp35* double mutant phenotype. As for the point mutation in *ada-2*, RNAi-based depletion of ADA-2 in *puf-8(zh17)* worms did not enhance the *puf-8* phenotype. Consistently, a transgene that expresses ADA-2 in the germline did not suppress the *puf-8(zh17) kp35* double mutant phenotype. Thus *kp35* is unlikely a mutant allele of either *him-14* or *ada-2*. By contrast, depletion of FARL-11 in *puf-8(zh17)* worms by RNAi caused sterility, and unlinking of the *farl-11* point mutation from *puf-8(zh17)* suppressed the *puf-8(zh17) kp35* double mutant phenotype

(Fig. S1 and data not shown). Further, the expression of a *farl-11* transgene in the germline restored fertility to *puf-8(zh17) kp35* double mutant worms (Fig. S1).

### Construction of transgenes

**pPK55** – expresses GFP::H2B fusion under the control of *pie-1* promoter and *farl-11* 3' UTR.

The *farl-11* 3' UTR was PCR-amplified from wild-type genomic DNA using PCR primers KS3965 and KS3966 (see Table S2 for primer sequences), and inserted at the Bsp120I site in pKS114 (Ariz et al., 2009).

**pPK57** – expresses GFP::FARL-11 fusion under the control of *pie-1* promoter and *tbb-2* (tubulin) 3' UTR. The *tbb-2* 3' UTR was PCR-amplified using PCR primers KS4092 and KS4093 from wild-type genomic DNA and inserted at Bsp120I site in pPK23, which carries the *pie-1* promoter and GFP-coding sequences upstream of the SpeI site. In addition, pPK23 backbone contains a 5.6-kb genomic DNA fragment that rescues the *unc-119(ed3)* defect. In the resulting plasmid, the 3466-bp FARL-11-coding sequences were PCR-amplified in two parts using primers KS4094-KS4095 and KS4096-KS4097 and inserted between SpeI-SacI and SacI-NarI sites, respectively.

**pRM62** – expresses FARL-11::GFP under the control of *farl-11* promoter and 3' UTR.

The *pie-1* promoter, GFP- and FARL-11-coding sequences and *tbb-2* 3' UTR in pPK57 plasmid were removed by digesting with NotI and KpnI. A 2975-bp genomic fragment immediately upstream of FARL-11-coding sequence was PCR-amplified using primers KS4190 and KS4191 and ligated between NotI and KpnI sites in the vector backbone generated above. The 3472-bp FARL-11-coding sequence was PCR-amplified using primers KS4192 and KS4193 and inserted at the SpeI site introduced by KS4191. The GFP-coding sequence was PCR-amplified from pPK55 using primers KS4194 and KS4195 and inserted at the Cfr9I site introduced by KS4193.



A 2815-bp genomic sequence immediately downstream of the FARL-11 stop codon was PCR-amplified using KS4196 and KS4197 and cloned between NarI and KpnI sites introduced by KS4195.

All constructs were made in duplicate and were introduced into the *unc-119(ed3)* strain by biolistic bombardment as described (Praitis et al., 2001) with modifications (Jadhav et al., 2008). Results presented in this study are representative of at least 20 worms from each of 3 independent transgenic lines.

## SUPPLEMENTARY FIGURES

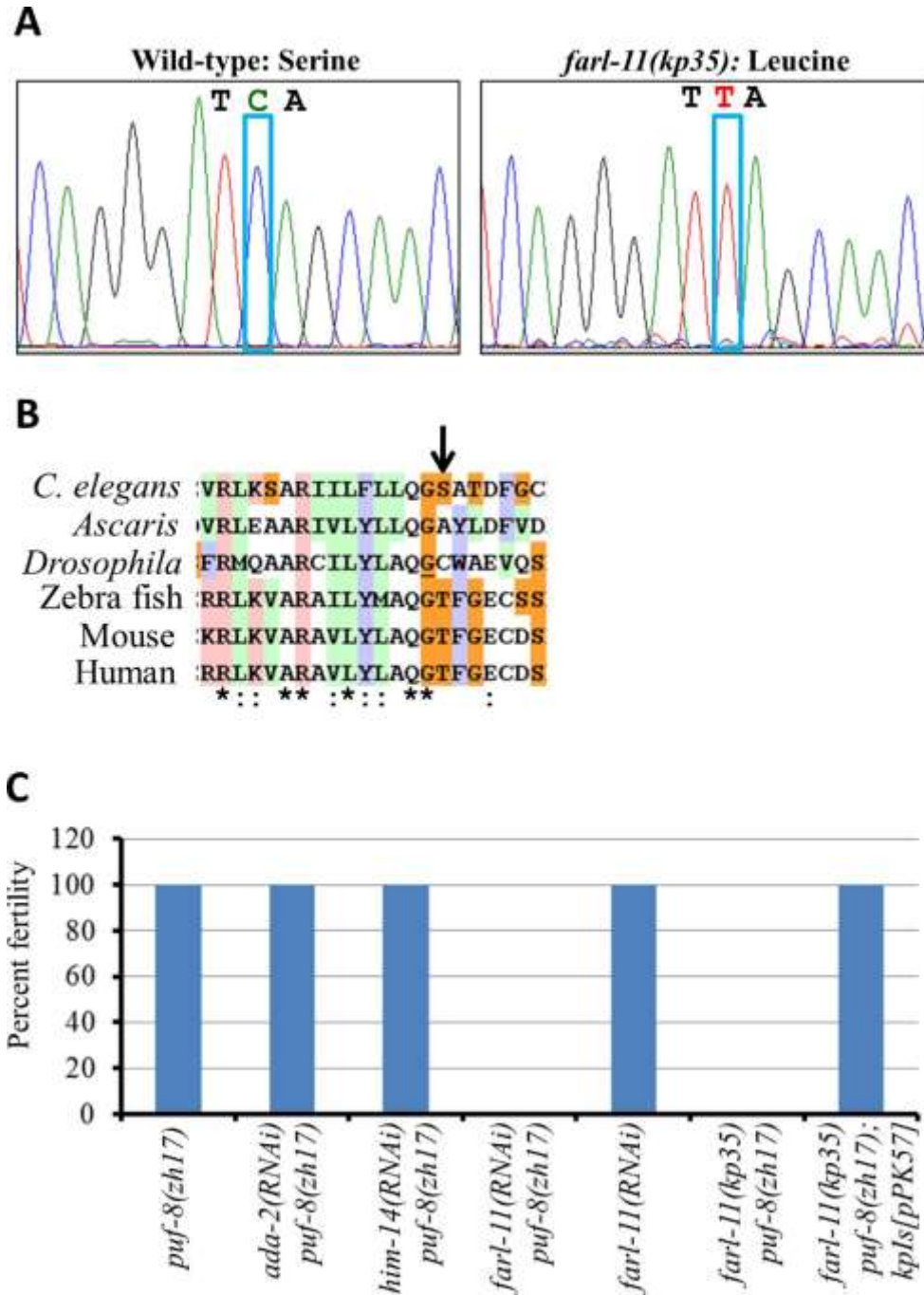


**Fig. S1. *kp35* is an allele of *farl-11*.** (A) Comparison of the wild-type and *kp35* electropherograms reveal a C-to-T substitution in the *farl-11* coding region. This single-base

mutation substitutes the semi-conserved [see **(B)**] serine residue at position 169 with leucine.

**(B)** Alignment of the FARL-11 amino acid sequence around the region bearing the *kp35*

mutation. The perfectly conserved residues are indicated with an asterisk (\*) at the bottom of

alignment and the double-dots indicate highly-conserved amino acid residues. **(C)** Bar graph

showing the percent of adult hermaphrodites, grown at 20°C, bearing gametes. In case of RNAi

treatment, results represent the adult progeny of RNAi-treated worms. *farl-11(RNAi) puf-*

*8(zh17)* and *farl-11(kp35) puf-8(zh17)* did not produce sperm or oocytes; *him-14(RNAi) puf-*

*8(zh17)* worms, although produced both types of gametes, laid mostly dead embryos, which is a

known phenotype of *him-14* mutants (Zalevsky et al., 1999). Animals of the other indicated

genotypes yielded viable embryos. *kpIs[pPK57]* is the *farl-11(kp35)*-rescuing transgene (strain

IT775; see Table S1 for complete description of the genotype). In each case, 100 adults were

examined per experiment, and the experiments were repeated four times.



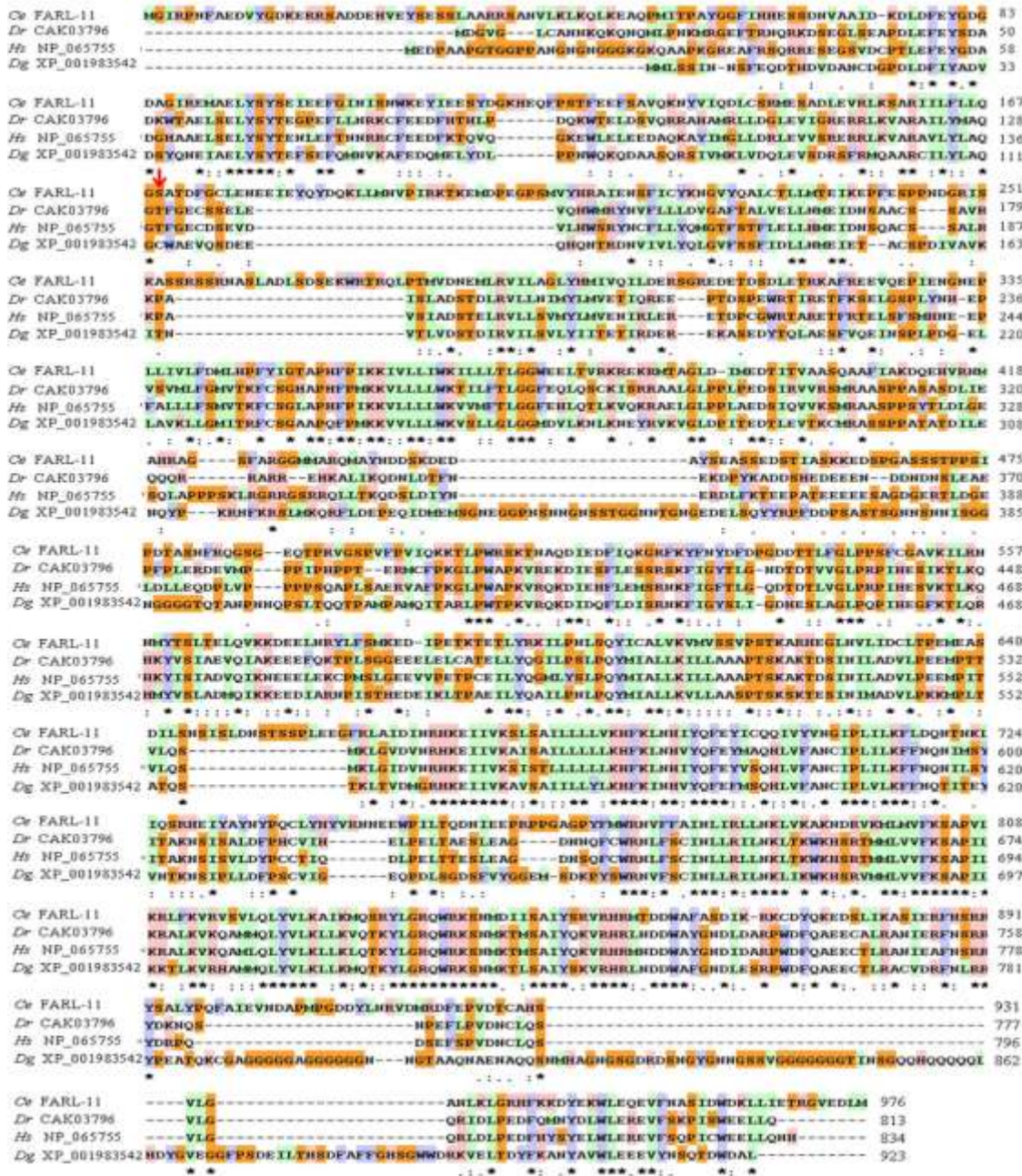


**Fig. S2. FARL-1 is a highly conserved protein.** Multiple sequence alignment shows alignment of *C. elegans* FARL-1 and its orthologs from human (*Hs* NP\_065755), Zebrafish (*Dr* CAK03796) and *Drosophila* (*Dg* XP\_001983542). E-values for the similarity between *C.*

*elegans* and the other species are: human –  $2 \times 10^{-150}$ , zebrafish –  $2 \times 10^{-149}$  and *Drosophila* –  $3 \times 10^{-137}$ . The protein sequences were aligned using the CLUSTALW program supplied with the DNA DYNAMO software package. Asterisk (\*) – identical amino acid in all aligned sequences; two dots (:) and single dot (.) – amino acids with very similar or somewhat similar side chains, respectively. The serine residue substituted in *kp35* with leucine is indicated by a red arrow.

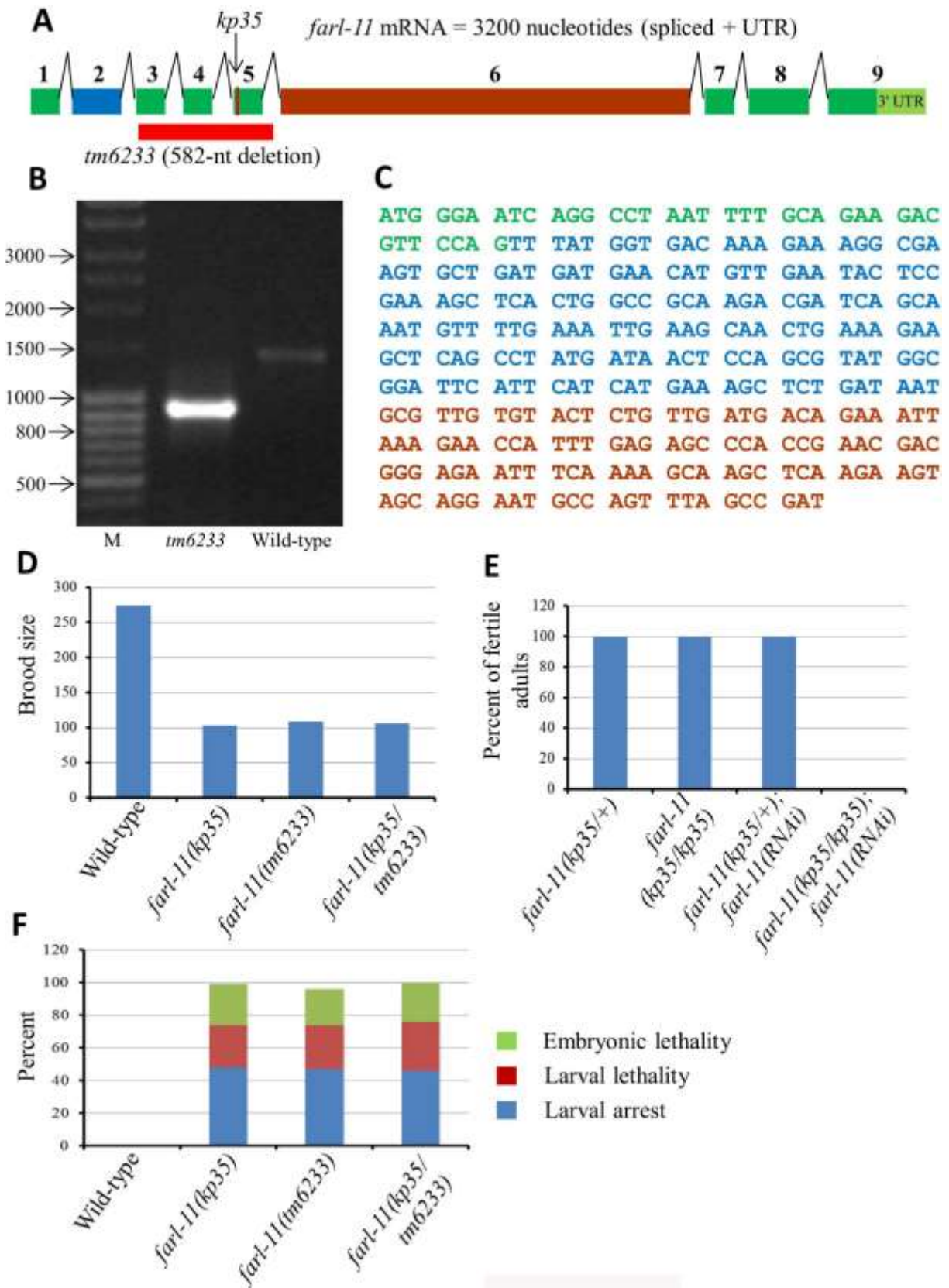




**Fig. S3. *kp35* and *tm6233* are hypomorphic alleles of *farl-11*.** (A) Schematic showing the positions of *kp35* and *tm6233* mutations. Colored bars with numbers represent the exons; exons 2 and 6 are shown in different colors to highlight the splicing observed in the *farl-11(tm6233)* worms [strain IT944], in which exons 3-5 are skipped. (B) Results of RT-PCR amplification of a product spanning exons 1-6 from *farl-1(tm6233)* and wild-type worms. Lane M – molecular weight markers; molecular size, in base-pairs, is shown on the left. (C) Nucleotide sequence of a part of the RT-PCR product amplified from *farl-1(tm6233)* worms, revealing the absence of exons 3-5 and the in-frame fusion of exon 2 and 6. (D) Bar graph showing the number of embryos per animal (brood size) of the indicated genotypes; values are average from 20 animals. Note: in D, E and F, the animals homozygous for the mutant allele are homozygous progeny of heterozygous mothers. As shown in F, most progeny of worms homozygous for *kp35* or *tm6233* fail to reach adulthood. (E) Percent of adult hermaphrodites, grown at 25°C, which produced embryos. Note that the *farl-11(kp35)* worms [strain IT719] are fertile, whereas the *farl-11(kp35)* worms fed with *farl-11* dsRNA produced sterile progeny. (F) Distribution of the various phenotypes observed among the progeny of animals of the indicated genotypes. Note that all three allelic combinations show similar phenotypes, indicating that 1) *kp35* and *tm6233* do not complement and 2) *tm6233* is also a hypomorphic allele. Error bars represent standard deviation.

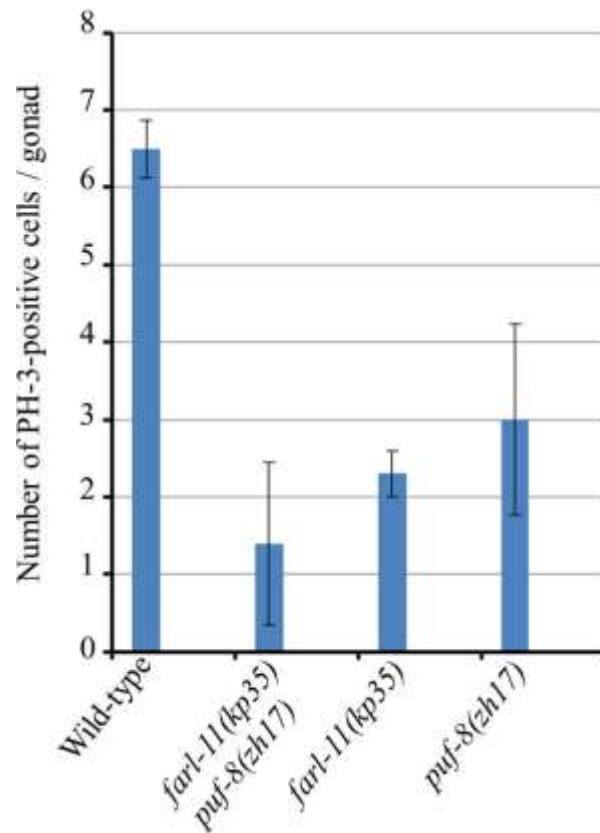


**Fig. S4. Quantitation of mitotically-dividing cells at the L4 larval stage.** Germlines of the indicated genotypes were immunostained with anti-PH3 antibody and the PH3-positive cells were counted. Error bars represent standard deviation and the P values calculated using the Student's t-test were less than 0.0001 for the difference between the wild-type and each of the three mutant genotypes.

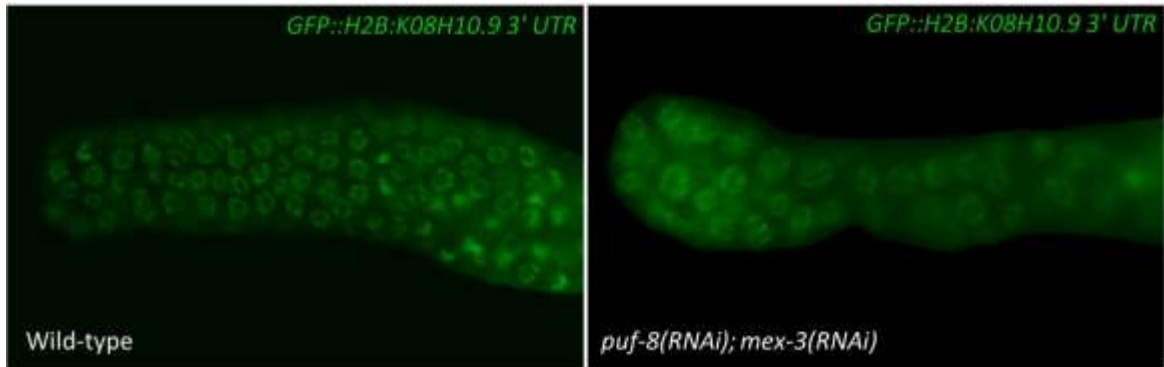


**Fig. S5. Depletion of PUF-8 and MEX-3 does not disrupt translational globally.** Expression pattern of the GFP::H2B fusion protein under the control of *pie-1* promoter and *K08H10.9 3' UTR* in the germlines of indicated genotypes. Scale bar: 20 $\mu$ m.



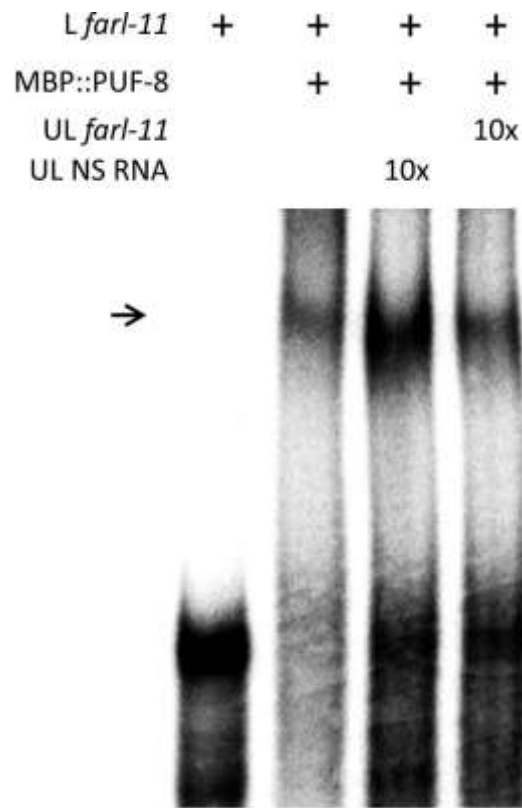


**Fig. S6. PUF-8 interacts with *farl-11* 3' UTR in vitro.** Electrophoretic mobility patterns of radiolabeled *farl-11* 3' UTR RNA (L *farl-11*) in the presence of the indicated components. MBP::PUF-8 – bacterially-expressed fusion protein containing maltose-binding protein and the PUF domain (175-535 amino acids) of PUF-8; UL – non-radiolabeled; NS – a non-specific RNA of about 200 nucleotides; 10x– 10 times molar excess compared to the radiolabeled RNA. Arrow indicates the mobility-shifted band.

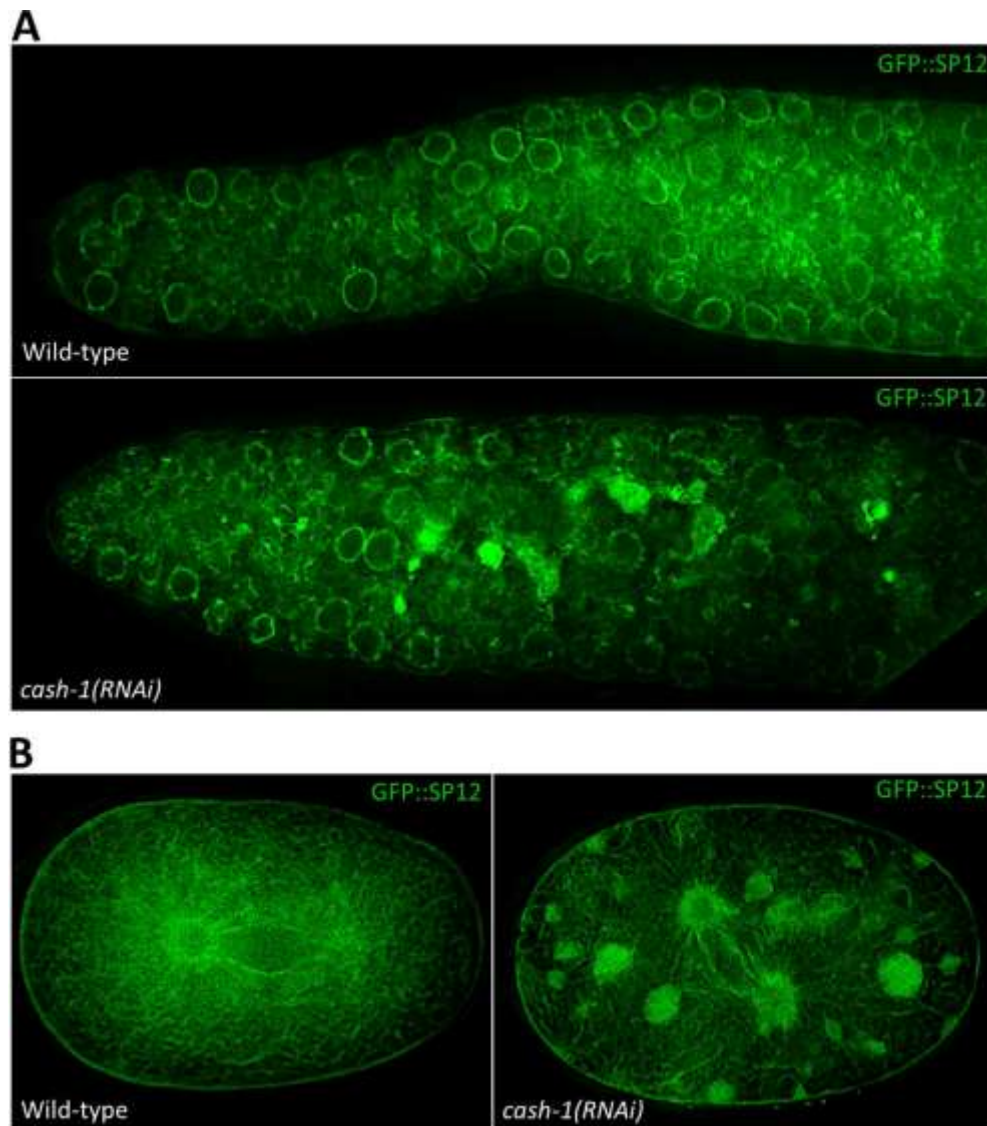


**Fig. S7. CASH-1 is essential for normal ER dynamics.** Distribution patterns of the ER marker GFP::SP12 in the distal germline (A) and the 1-cell embryo at first metaphase (B) [strain SP12]. In the CASH-1 depleted germline and embryo, ER forms large cytoplasmic patches similar to the *farl-11* mutant (see Fig. 7). Scale bar: 20 $\mu$ m.

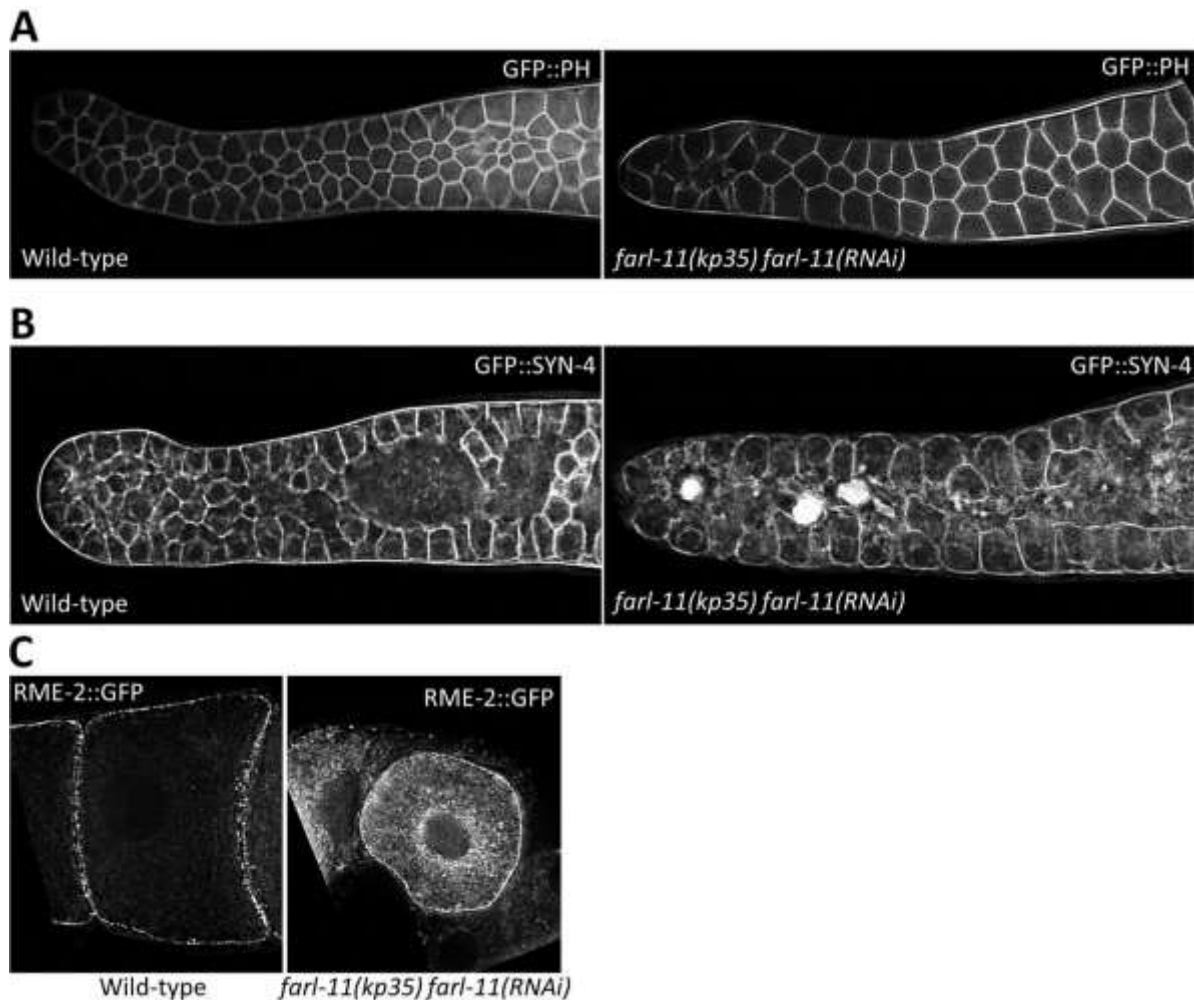


**Fig. S8. Loss of *farl-11* activity affects protein transport and ER, but not the plasma membrane.** (A) Germ cell membranes in the distal germline, visualized by expression of the membrane marker GFP::PH, are unaffected by the depletion of FARL-11 (right panel) [strains OD58 and IT933]. In contrast, the syntaxin GFP::SYN-4 forms large aggregates, similar to GLP-1 (Fig. 9), in the lumen of FARL-11-depleted distal germlines (B) [strains FT204 and IT1083]. Although the pleckstrin homology domain-containing proteins (GFP::PH) and

syntaxins bypass the ER-dependent protein transport pathway and are directly inserted into plasma membrane, only syntaxins are inserted into the ER membrane as well (Kutay et al., 1993; Wang and Shaw, 1995). (C) Expression pattern of RME-2::GFP – RME-2 is a yolk receptor – in oocytes. The rectangular structure on the left image is a single wild-type oocyte, in which RME-2::GFP is seen only on the cell membrane [strain RT408]. In contrast, in the FARL-11-depleted oocyte [strain IT1081], besides being on the cell membrane, it appears as a halo of granules around the nucleus, suggesting defects in its transport to the plasma membrane. Note: While *farl-11(kp35)* worms grown at 20°C form large oocytes (Fig. 8 D), *farl-11(kp35) farl-11(RNAi)* worms grown at 20°C form a few smaller oocytes like the one shown here. Scale bar: 20µm.



**Table S1. *C. elegans* strains used in this study**

Strain name	Genotype	Reference
IT729	<i>unc-119(ed3) III; kpIs(pPK55) [Ppie-1::gfp::his-58::farl-11 3' UTR; unc-119(+)]</i>	This study
IT735	<i>puf-8(ok302) unc-4(e120) / mnC1 II; kpIs(pPK55)</i>	This study
IT767	<i>mex-3(zu155) dpy-5(e61) / hT1 I; kpIs(pPK55)</i>	This study
IT773	<i>unc-119(ed3) III; kpIs(pPK57) [Ppie-1::gfp::farl-11::tbb-2 3' UTR; unc-119(+)]</i>	This study
IT775	<i>farl-11(kp35) puf-8(zh17) unc-4(e120) / mnC1 II; kpIs(pPK57)</i>	This study
IT807	<i>unc-119(ed3) III; kpIs(pRM62) [Pfarl-11::farl-11::gfp::farl-11 3' UTR; unc-119(+)]</i>	This study
IT853	<i>puf-8(ok302) unc-4(e120) / mnC1 II; kpIs(pRM62)</i>	This study
IT854	<i>farl-11(kp35) puf-8(zh17) unc-4(e120) / mnC1 II; kpIs(pRM62)</i>	This study
SP12	<i>unc-119(ed3) III; Ppie-1::gfp::SP12::pie-1 3' UTR; unc-119(+)</i>	(Poteryaev et al., 2005)
OD139	<i>unc-119(ed3) III; ltIs37 [Ppie-1::mCherry::his-58; unc-119 (+)] IV; qaIs3502 [Ppie-1::yfp::lmn-1; unc-119(+)]</i>	(Portier et al., 2007)
IT935	<i>puf-8(ok302) / mnC1 II; Ppie-1::gfp::SP12::pie-1 3' UTR; ltIs37 [GFP::SP12 + mCherry::H2B]</i>	This study
IT936	<i>farl-11(kp35) rol-6 (e187) / mnC1 II; Ppie-1::gfp::SP12::pie-1 3' UTR; ltIs37 [GFP::SP12 + mCherry::H2B]</i>	This study
IT938	<i>farl-11(kp35) puf-8 (zh17) unc-4(e120) / mnC1 II; Ppie-1::gfp::SP12::pie-1 3' UTR; ltIs37 [GFP::SP12 + mCherry::H2B]</i>	This study
OCF15	<i>unc-119(ed3) III; ocfIs2 [Ppie-1::mCherry::SP12::pie-1 3' UTR; unc-119(+)]</i>	(Joseph-Strauss et al., 2012)
IT939	<i>unc-119(ed3) III; ocfIs2; kpIs(pRM62) [mCherry::SP12 + FARL-11::GFP]</i>	This study
IT940	<i>unc-119(ed3) III; kpIs(pRM62); ltIs37 [FARL-11::GFP + mCherry::H2B]</i>	This study
IT722	<i>unc-119(ed3) III; kpIs(pAK9) [Ppuf-8::puf-8::9xHA::gfp::puf-8 3' UTR]</i>	(Vaid et al., 2013)
IT305	<i>unc-119(ed3) III; kpIs(pPK19) [Ppie-1::mCherry::emr-1::hip-1 3' UTR; unc-119(+)]</i>	(Pushpa et al., 2013)
OD58	<i>unc-119(ed3) III; ltIs38 [Ppie-1::gfp::PH(PLC1delta1) + unc-119(+)].</i>	(Audhya et al., 2005)
IT933	<i>farl-11(kp35) rol-6(e187) / mnC1 II; ltIs38</i>	This study
IT867	<i>unc-119(ed3) III; kpIs(pRM62);kpIs(pPK19) [FARL-11::GFP + mCherry::EMR-1]</i>	This study

FT204	<i>unc-119(ed3) III; xnIs87 [Psyn-4::gfp::syn-4::syn-4 3' UTR + unc-119(+)]</i>	From Caenorhabditis Genetics Center (CGC) strain data
IT1083	<i>farl-11(kp35) rol-6(e187) / mnC1 II; xnIs87</i>	This study
RT408	<i>unc-119(ed3) III; pwIs116 [Prme-2::rme-2::gfp::rme-2 3' UTR + unc-119(+)]</i>	(Balklava et al., 2007)
IT1081	<i>farl-11(kp35) rol-6(e187) / mnC1 II; pwIs116</i>	This study
IT60	<i>puf-8(zh17) unc-4(e120) / mnC1 II</i>	(Ariz et al., 2009)
JH1500	<i>puf-8(ok302) unc-4(e120) / mnc1 II</i>	(Subramaniam and Seydoux, 2003)
IT719	<i>farl-11(kp35) rol-6(e187) / mnC1 II</i>	This study
EW23	<i>unc-104(e1265) rol-6(e187) II</i>	From CGC strain data
IT175	<i>farl-11(kp35) puf-8(zh17) unc-4(e120) / mC6g II</i>	This study
IT73	<i>farl-11(kp35) puf-8(zh17) rol-6(e187) / mnC1 II</i>	This study
IT944	<i>farl-11(tm6233) / mIn1 II</i>	From National BioResource Project, Japan
JK509	<i>glp-1(q231) III</i>	(Austin and Kimble, 1987)
GC833	<i>glp-1(ar202) III</i>	(Pepper et al., 2003)
IT870	<i>farl-11(kp35) rol-6(e187) / mnC1 II; glp-1(q231) III</i>	This study
IT871	<i>farl-11(kp35) rol-6(e187) / mnC1 II; glp-1(ar202) III</i>	This study
IT135	<i>unc-104(e1265) puf-8(zh17) rol-6(e187) II</i>	This study
DR2078	<i>mIn1[dpy-10(e128) mIs14] / bli-2(e768) unc-4(e120) II</i>	From CGC strain data

---

**Table S2. Oligonucleotide PCR primers used in this study**

Primer name	Sequence	Description
KS1102	TCTAAGCTTATGGCTCAAACAAAGCCGAT	Forward for <i>pie-1</i> mRNA
KS2495	AATCTGACGACGATTCGAGC	Reverse for <i>pie-1</i> mRNA
KS2808	CCAAGGGGTTATGCTAGGAAG	Forward primer for synthesizing in vitro transcription template
KS3949	ACATCCAAAGTCTGTTGCTA	Reverse primer carrying the <i>kp35</i> mutation
KS3950	TGAAAGAAGCTCAGCCTATG	Forward primer about 500 bases upstream of KS3949
KS3965	TCTGCAGGGCCCATCGATTCGATCCCGTTTCC	Forward primer for <i>farl-11</i> 3' UTR
KS3966	TCTGCAGGGCCCGTGAGTCTGGATACCCGAAG	Reverse primer for <i>farl-11</i> 3' UTR
KS4092	TCTGCAGGGCCCATGCAAGATCCTTTCAAGCA	Forward primer tubulin <i>tbb-2</i> 3' UTR
KS4093	TCTGCAGGGCCCTGAGACTTTTTTCTTGCCGG	Reverse primer tubulin <i>tbb-2</i> 3' UTR
KS4094	TCTGCAACTAGTGGAATCAGGCCTAATTTTGC	Forward primer for the FARL-11-coding region fragment-1
KS4095	GCAATCGTTGAGTCTTCGGA	Reverse primer for the FARL-11-coding region fragment-1
KS4096	GAAGACGCTTATTCGGAAGC	Forward primer for the FARL-11-coding region fragment-2
KS4097	TCTGCAGGCGCCTTACATAAGATCTTCCACTCCAC GTG	Reverse primer for the FARL-11-coding region fragment-2
KS4190	TCTGCAGCGGCCGCCACAAGGCCCATTTTCTGCG	Forward primer for <i>farl-11</i> upstream
KS4191	TCTGCAGGTACCACTAGTTATATTACTAGTCATTT TCTCACCGTCTTCTGC	Reverse primer for <i>farl-11</i> upstream
KS4192	TCTGCAACTAGTAATATATCATCAAATAAACCTCC TAATAGTTCCAGTTTATGGTGACAAAGAAAGGCG	Forward primer for the FARL-11-coding region
KS4193	TCTGCAGGTACCCCCGGGCATAAGATCTTCCACTC CACG	Reverse primer for the FARL-11-coding region

KS4194	TCTGCACCCGGGATGAGTAAAGGAGAAGAACT	Forward primer for GFP
KS4195	TCTGCAGGTACCGGCCTTATTTGTATAGTTCAT CCATGCC	Reverse primer for GFP
KS4196	TCTGCAGGCGCCATCGATTCGATCCCGTTTCC	Forward primer for <i>farl-11</i> downstream
KS4197	TCTGCAGGTACCTGTGGCGCACAGGATATCTC	Reverse primer for <i>farl-11</i> downstream
KS4252	TATGTAAACAATTGAATTCATTCGG	Reverse primer for <i>farl-11</i> 3' UTR



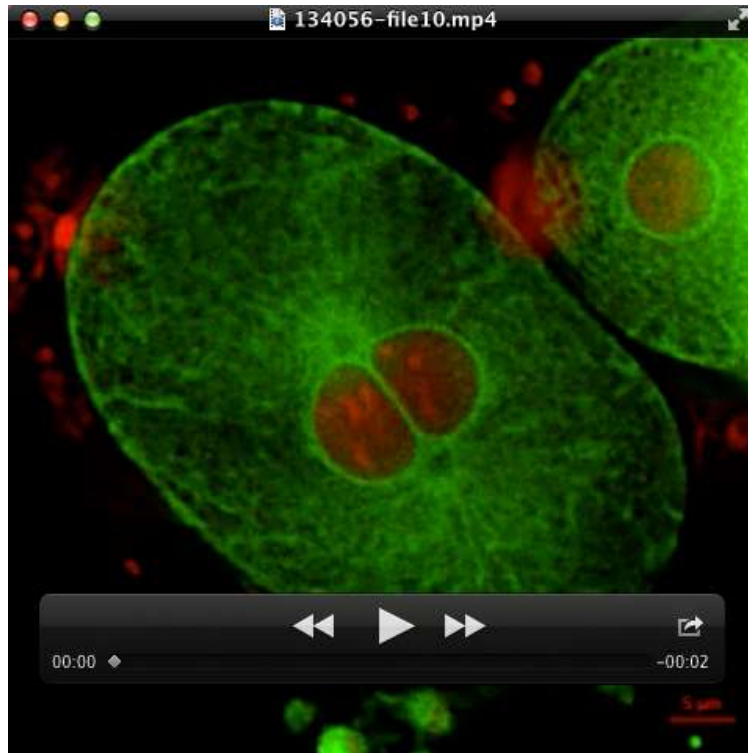
## SUPPLEMENTARY REFERENCES

- Ariz, M., Mainpal, R. and Subramaniam, K.** (2009). *C. elegans* RNA-binding proteins PUF-8 and MEX-3 function redundantly to promote germline stem cell mitosis. *Dev. Biol.* **326**, 295-304.
- Audhya, A., Hyndman, F., McLeod, I. X., Maddox, A. S., Yates, J. R., 3rd, Desai, A. and Oegema, K.** (2005). A complex containing the Sm protein CAR-1 and the RNA helicase CGH-1 is required for embryonic cytokinesis in *Caenorhabditis elegans*. *J. Cell Biol.* **171**, 267-79.
- Austin, J. and Kimble, J.** (1987). *glp-1* is required in the germ line for regulation of the decision between mitosis and meiosis in *C. elegans*. *Cell* **51**, 589-99.
- Balklava, Z., Pant, S., Fares, H. and Grant, B. D.** (2007). Genome-wide analysis identifies a general requirement for polarity proteins in endocytic traffic. *Nat. Cell Biol.* **9**, 1066-73.
- Jadhav, S., Rana, M. and Subramaniam, K.** (2008). Multiple maternal proteins coordinate to restrict the translation of *C. elegans* *nanos-2* to primordial germ cells. *Development* **135**, 1803-12.
- Joseph-Strauss, D., Gorjanacz, M., Santarella-Mellwig, R., Voronina, E., Audhya, A. and Cohen-Fix, O.** (2012). Sm protein down-regulation leads to defects in nuclear pore complex disassembly and distribution in *C. elegans* embryos. *Dev. Biol.* **365**, 445-57.
- Kutay, U., Hartmann, E. and Rapoport, T. A.** (1993). A class of membrane proteins with a C-terminal anchor. *Trends Cell Biol.* **3**, 72-5.
- Pepper, A. S., Killian, D. J. and Hubbard, E. J.** (2003). Genetic analysis of *Caenorhabditis elegans* *glp-1* mutants suggests receptor interaction or competition. *Genetics* **163**, 115-32.
- Portier, N., Audhya, A., Maddox, P. S., Green, R. A., Dammermann, A., Desai, A. and Oegema, K.** (2007). A microtubule-independent role for centrosomes and aurora a in nuclear envelope breakdown. *Dev. Cell* **12**, 515-29.
- Poteryaev, D., Squirrell, J. M., Campbell, J. M., White, J. G. and Spang, A.** (2005). Involvement of the actin cytoskeleton and homotypic membrane fusion in ER dynamics in *Caenorhabditis elegans*. *Mol. Biol. Cell* **16**, 2139-53.
- Praitis, V., Casey, E., Collar, D. and Austin, J.** (2001). Creation of low-copy integrated transgenic lines in *Caenorhabditis elegans*. *Genetics* **157**, 1217-26.
- Pushpa, K., Kumar, G. A. and Subramaniam, K.** (2013). PUF-8 and TCER-1 are essential for normal levels of multiple mRNAs in the *C. elegans* germline. *Development* **140**, 1312-20.
- Subramaniam, K. and Seydoux, G.** (2003). Dedifferentiation of primary spermatocytes into germ cell tumors in *C. elegans* lacking the pumilio-like protein PUF-8. *Curr. Biol.* **13**, 134-9.
- Vaid, S., Ariz, M., Chaturvedi, A., Kumar, G. A. and Subramaniam, K.** (2013). PUF-8 negatively regulates RAS/MAPK signalling to promote differentiation of *C. elegans* germ cells. *Development* **140**, 1645-54.

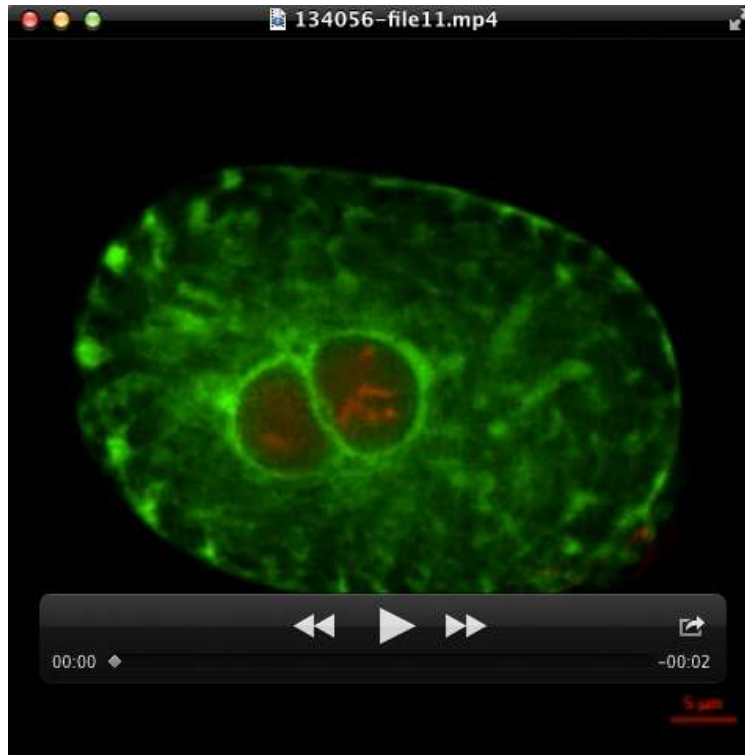
**Wang, D. S. and Shaw, G.** (1995). The association of the C-terminal region of beta I sigma II spectrin to brain membranes is mediated by a PH domain, does not require membrane proteins, and coincides with a inositol-1,4,5 triphosphate binding site. *Biochem. Biophys. Res. Commun.* **217**, 608-15.

**Zalevsky, J., MacQueen, A. J., Duffy, J. B., Kempfues, K. J. and Villeneuve, A. M.** (1999). Crossing over during *Caenorhabditis elegans* meiosis requires a conserved MutS-based pathway that is partially dispensable in budding yeast. *Genetics* **153**, 1271-83.

## MOVIES

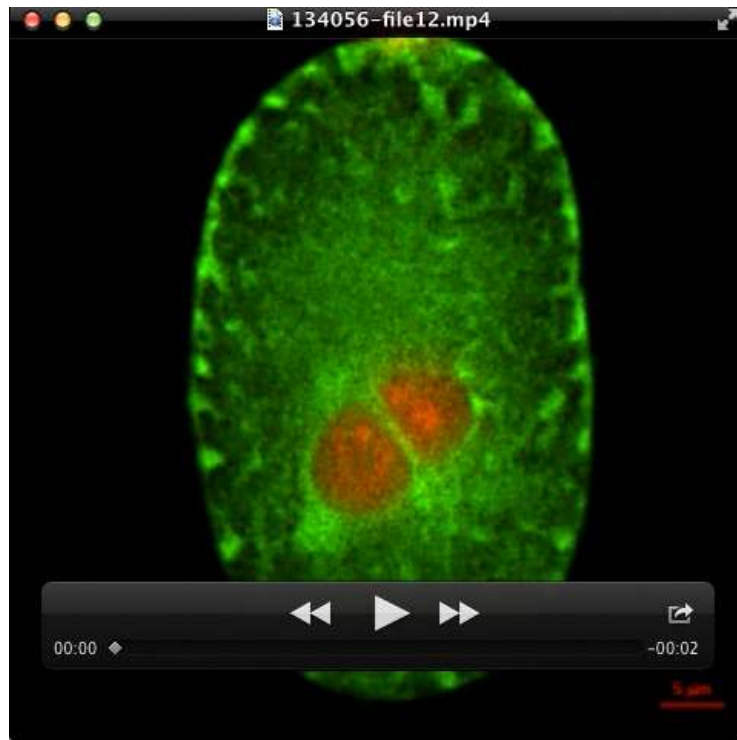


**Movie 1. ER dynamics during the first mitotic division of the wild-type embryo.** Time-lapse movie of 1-cell embryo expressing the ER marker GFP::SP12 and the chromatin marker mCherry::H2B. The embryo was imaged every 1 minute for 17 minutes, and the images were deconvolved as described in Materials and methods and played at 5 frames / second.



**Movie 2. ER dynamics during the first mitotic division of the *far1-11(kp35)* embryo.** Time-lapse movie of 1-cell embryo expressing the ER marker GFP::SP12 and the chromatin marker mCherry::H2B. The embryo was imaged every 1 minute for 17 minutes, and the images were deconvolved as described in Materials and methods and played at 5 frames / second.





**Movie 3. ER dynamics during the first mitotic division of the *puf-8(zh17)* embryo.** Time-lapse movie of 1-cell embryo expressing the ER marker GFP::SP12 and the chromatin marker mCherry::H2B. The embryo was imaged every 1 minute for 17 minutes, and the images were deconvolved as described in Materials and methods and played at 5 frames / second.